Spectral Index and Quasi-Periodic Oscillation Frequency Correlation in Black Hole (BH) Sources: Observational Evidence of Two Phases and Phase Transition in BHs

Lev Titarchuk[1,2,4] and Ralph Fiorito [3,4]

ABSTRACT

Recent studies have shown that strong correlations are observed between the low frequencies (1-10 Hz) of quasiperiodic oscillations (QPOs) and the spectral power law index of several Black Hole (BH) candidate sources, in low hard states, steep power-law (soft) states and in transition between these states. The observations indicate that the X-ray spectrum of such state (phases) show the presence of a power-law component and are sometimes related to simulataneous radio emission indicated the probable presence of a jet. Strong QPOs ($> 20\%$ rms) are present in the power density spectrum in the spectral range where the power-law component is dominant (i.e. 60-90%). This evidence contradicts the dominant long standing interpretation of QPOs as a signature of the thermal accretion disk. We present the data from the literature and our own data to illustrate the dominance of power-law index-QPO frequency correlations. We provide a model, that identifies and explains the origin of the QPOs and how they are imprinted on the properties of power-law flux component. We argue the existence of a bounded compact coronal region which is a natural consequence of the adjustment of Keplerian disk flow to the innermost sub-Keplerian boundary conditions near the central object and that ultimately leads to the formation of a transition layer (TL) between the adjustment radius and the innermost boundary. The model predicts two phases or states dictated by the photon upscattering produced in the TL: (1) hard state, in which the TL is optically thin and very hot ($kT \gtrsim 50$ keV) producing photon upscattering via thermal Componization; the photon spectrum index $\Gamma \sim 1.5$ for this state is dictated by gravitational energy release and Compton cooling in an optically thin shock near the adjustment

[1]George Mason University/SCS/CEOSR, Fairfax VA 22030; lev@xip.nrl.navy.mil

[2]Naval Research Laboratory, Washington DC; lev@xip.nrl.navy.mil

[3]University of Maryland, College Park USA

[4]NASA/ Goddard Space Flight Center, Greenbelt MD 20771, USA

radius; (2) a soft state which is optically thick and relatively cold ($kT \lesssim 5$ keV); the index for this state, $\Gamma \sim 2.8$ is determined by soft-photon upscattering and photon trapping in converging flow into BH. In the TL model for corona the QPO frequency ν_{high} is related to the gravitational (close to Keplerian) frequency $\nu_{\rm K}$ at the outer (adjustment) radius and ν_{low} is related to the TL's normal mode (magnetoacoustic) oscillation frequency ν_{MA}. The observed correlations between index and low and high QPO frequencies are readily explained in terms of this model. We also suggest a new method for evaluation of the BH mass using the index-frequency correlation.

1. Introduction

The short dynamical time scales and coherence of quasi-periodic oscillations (QPOs) observed in accreting XRB's strongly suggest that QPOs can provide valuable information on the accretion dynamics in the innermost parts of these systems. In this respect the discovery of low 20-50 Hz QPOs in luminous neutron star (NS) binaries by van der Klis et al. (1985), kilohertz QPOs in NS's by Strohmayer et al. (1996) and hectohertz QPO's in BH's by Morgan, Remillard & Greiner (1997) opened a new era in the study of the dynamics near compact objects. Following these discoveries Psaltis, Belloni & van der Klis (1999), hereafter PBK, demonstrated that these NS and BH low and high frequencies follow a remarkably tight correlation. These features are the "horizontal branch oscillations" (HBO) along with "low frequency noise Lorentzian", ν_{low} and the lower kHz QPO ν_{high} for NS and BH respectively. Belloni, Psaltis & van der Klis (2002), hereafter BPK, have updated PBK's correlation adding data from Nowak (2000), Boirin et al. (2000), Homan et al. (2001), Di Salvo et al. (2001) and Nowak et al. (2002). PBK suggest that the low and high frequencies correlate in a way that seems to depend only weakly on the properties of the sources, such the mass, magnetic field, or possibly the presence of a hard surface in compact object. Mauche (2002) has reported low and high frequency QPO's in the dwarf nova SS Cygni and VW Hyi (see Wouldt & Warner 2002 for for the VW Hyi observations) and has called attention to the fact that these QPO's extend the correlation of PBK downward in frequency by more than two orders of magnitude This frequency correlation observed over such a broad range of sources indicates that a common phenomenon is responsible for QPOs in compact objects and raises the question whether one can find a observational relations which would distinguish BH candidates from other compact sources.

The comparative study of spectral and QPO features in BH candidate sources has yielded important information which can help answer this question. As far as spectral

properties are concerned, there is increasing observational evidence that the large complex of spectral "states" originally devised by Belloni (2000) to classify the highly variable X-ray spectra of BH galactic sources like GRS 1915+105, can be reduced to a few simple configurations [see e.g. McClintock and Remillard (2003) and Belloni (2003)]: (1) a low hard power law dominated state where the photon spectral index is near 1.5; (2) a steep power law state in which the index is about 2.7; (3) and a thermally dominated state. The observed variability is explained by transitions between these three canonical configurations.

Low frequency (1-10 Hz) QPO's are generally observed to present in states (1) and (2), during transitions between states (1) and (2) but never in (3). Both high and low frequency QPO's have been thought to be associated with the accretion disk, though their specific origin has not widely understood (although see Titarchuk & Wood 2002, hereafter TW02, for explanation of their origin). Attempts to find consistent correlations with observable disk parameters have lead to mixed results. In particular, there are so many exceptions to the observed correlations of frequency to disk spectral values sometimes observed that no general statement about the relation of the QPO with any spectral parameter solely associated with the disk, such as thermal flux, temperature, inner radius, etc. can be made. For example, exceptions to one of the most widely quoted correlations, i.e. between disk flux and frequency, have been presented for the well studied micro-quasar GRS 1915+105 by Fiorito, Markwardt, & Swank (2003) and for XTE 1550-564 by Remillard et. al. (2002).

On the other hand, a number of recent studies have revealed consistent and robust correlations between the photon index of the power-law component of the X-ray spectrum and low QPO frequency. Such strong correlations are observed the well-studied BH binary, GRS 1915+105 in almost all situations in which the QPO is observable and in several other BH's over a wide range of observations and states.

These studies include:

a. A comprehensive study of correlations between photon index and QPO frequency in BH sources by Vignarca et al. (2003); these results show strong correlations between index and QPO frequency as well as saturation of the index between at the values 1.5 ± 0.1 and 2.7 ± 0.2 for several BH sources and for the same source in different states.

b. Recent studies by Kalemci (2002) for a number of galactic BH x-ray transients observed during outburst decay which confirm the persistence of the correlation between frequency and index during state transitions.

c. Our own studies of GRS 1915+105 of χ states (Fiorito, Markwardt, & Swank 2003), in which strong correlation of QPO frequency with power-law index have been observed; such states have been traditionally noted as low brightness, power law dominated states (see

e.g. Belloni et al. 1999) where the disk is at least tenuous if not undetectable altogether.

d. Studies tracing the QPO frequency and index over time between state transitions shows that the frequency tracks the index during state evolution (Homan, et. al. 2001) and Sobczak et al. (1999, 2000) from a value of about 1.5 ± 0.1 to about 2.7 ± 0.2, as the QPO frequency varies from about 1 to 10 Hz.

The persistence of the correlation of index with QPO frequency and its tracking with respect to time suggests that the underlying physical process or condition which gives rise to the low frequency QPO are tied to the corona, which gives rise to the power-law component, and furthermore, that this physical process or condition varies in a well defined manner as the source progresses from one state to another. Moreover, the fact that the same characteristics of the correlation are seen in so many galactic X-ray binary BH sources, which vary widely in both luminosity (presumably with mass accretion rate) and state, suggests that the physical processes controlling the index and the low frequency QPOs is a characteristic property of these sources, and by virtue of the observed correlations of PBK, may be a universal property of *all* accreting compact systems.

The above data have motivated us to develop a detailed model of the physics of the corona surrounding a BH s which directly predicts the behavior of the spectral index with fundamental properties of the corona. The model we have developed incorporates fundamental principles of fluid mechanics, radiative transfer theory and oscillatory processes. It identifies the origin of the QPO as a fundamental property of a compact coronal region near the BH and shows how the photon index of this corona changes as a function of mass accretion rate.

It has been already shown in a number of papers (see below) that the absence of the firm surface in the BHs leads to the development of the very strong converging flow when the mass accretion rate is higher than Eddington rate $\dot{M}_{Edd} = L_{Edd}/c^2$. The main observational features of the converging flow should be seen in high/soft phase, while the thermal Comptonization spectrum of the soft (presumably disk) photons should be seen in the hard phase.

In series of papers (Chakrabarti & Titarchuk 1995, hereafter CT95; Titarchuk, Mastichiadis & Kylafis 1996, 1997; Ebisawa, Titarchuk & Chakrabarti 1996; Titarchuk & Zannias 1998; Shrader & Titarchuk 1998, 1999; Borozdin et al. 1999; Laurent & Titarchuk 1999, 2001, hereafter LT99 and LT01 respectively; Titarchuk & Shrader 2002; Turolla, Zane & Titarchuk 2002) the authors argue that the drain properties of black horizon are necessarily related to the bulk inflow in BH sources and that the spectral and timing features of this bulk inflow are really detected in the X-ray observations of BHs. The signatures of the inflow are:

i. an extended steep power law where the photon index saturates to the value 2.7 ± 0.2 as the mass accretion rate increases - the precise value of the index is a function of the temperature of the flow but its relatively high value is a result of inefficient photon upscattering in the converging flow due to photon trapping. Moreover, LT99 demonstrated using Monte Carlo simulations that in the low hard state when the plasma temperature is of order 50 keV the bulk inflow spectrum is practically identical to thermal Comptonization spectrum (there is no any noticeable effect of the bulk Comptonization in the spectrum) and the spectral index varies in narrow range from 2 to 1.7 with mass accretion rate (in Eddington units) increases from 2 to 7. The similar small variation of the photon index around 1.7 in the low hard state was pointed out in earlier work by CT95. In fact, the effect of the bulk Comptonization compared to thermal one is getting stronger when the plasma temperature drops below 10 keV.

ii. the QPO high frequency (100-300 Hz), which is inversely proportional to BH mass; iii these two features are closely related but the variability of the soft spectral component is not correlated at all with the variability of the power law component.

Furthermore, Titarchuk, Osherovich & Kuznetsov (1999), hereafter TOK, presented observational evidence that the variability of the hard X-ray radiation in NS's and BH's occurs *in a bounded configuration.* Ford & van der Klis (1998) found that the break frequency in the power density spectrum (PDS) is correlated with QPO frequency for some particular NS sources (4U 1728-32). Wijnands & van der Klis (1999) later found a similar correlation in BH sources. Titarchuk & Osherovich (1999), hereafter TO99, and TOK explained this correlation in NSs and BHs respectively. They argue the observed PDS is the power spectrum of an exponential shot, $\exp(-t/t_d)$ which is the response of the diffusion propagation to any perturbation in a bounded medium. The inverse of the characteristic diffusion time $\nu_b = 1/t_d$ and the normal mode QPO frequency ν_0 has a well defined relation to the size of the bounded configuration, because $\nu_b \propto V/L$ and $\nu_0 \propto V/L^2$ where V is the specific pertrubation (magneto-sonic) velocity and L is a charactestic size of the configuration (see TO99).

Titarchuk, Lapidus & Muslimov (1998), hereafter TLM98 proposed that this bounded configuration (cavity) surrounding compact objects is the transition layer (TL) that is formed as a result of dynamical adjustments of a Keplerian disk to the innermost sub-Keplerian boundary conditions. They argued that this type of adjustment is a generic feature of the Keplerian flow in the presence of the sub-Keplerian boundary conditions near the central object and that it does not necessarily require the presence or absence of a hard surface. TLM98 concluded that an isothermal sub-Keplerian transition layer between the NS surface and its last Keplerian orbit forms as a result of this adjustment. The TL model is general and

is applicable to both NS and black hole systems. The primary problem in both NS and BH systems is understanding how the flow changes from pure Keplerian to the sub-Keplerian as the radius decreases to small values. TLM98 suggested that the discontinuities and abrupt transitions in their solution result from derivatives of quantities such as angular velocities (weak shocks). They were first to put forth the possibility of the transition layer formation to explain most observed QPOs in bright low mass X-ray binaries (LMXBs). In Figure 1 we illustrate the main idea of the transition layer concept for NS's ans BH's.

Subsequently, TO99 identified the transition layer (TL) model's corresponding viscous frequency ν_V and diffusion or break frequency ν_b for 4U 1728-34. The predicted values for ν_b related to diffusion in the transition layer. Then, TOK confirmed, with observations of a number of QPO sources (Wijnands et al. 1999), the relationship $\nu_b \propto \nu_V^{1.6}$, which is valid for both NS and BH candidate sources.

In this *Paper*, we explain the general correlation between photon index and low frequency in the frameworks of the transition layer model and we give more arguments for the nature of the spectral phases (states) and phase transition observed in BHCs. The main features of the TL model are given in §2.1. The formulation of the problem of low frequency oscillations and the relationship with MA oscillations in the transition layer are described in §2.2. The derivation of the low frequency-index correlation is present in §2.3. We give the details of modeling of the spectral phase transition in §2.4. In §3 we present and analyze specific QPO and spectral data in terms of the TL model. We discuss the signatures and the methods of the identification of BH and NS sources using timing and spectral characteristics in §4. Our summary and conclusions also follow in §4.

2. Transition Layer Theory

2.1. The main features of the transition layer model

TLM98 define the transition layer as a region confined between the the inner sub-Keplerian disk boundary and the first Keplerian orbit (for the TL geometry, see Fig. 1 and Fig. 1 in TLM98 and TOK). The radial motion in the disk is controlled by friction and the angular momentum exchange between adjacent layers, resulting in the loss of the initial angular momentum by accreting matter. The corresponding radial transport of the angular momentum in a disk is described by the following equation (see e.g. Shakura & Sunyaev 1973, hereafter SS73):

$$\dot{M}\frac{d}{dR}(\omega R^2) = 2\pi\frac{d}{dR}(W_{r\varphi}R^2), \tag{1}$$

where $\dot{M}$ is the accretion rate in the disk and $W_{r\varphi}$ is the component of a viscous stress tensor that is related to the gradient of the rotational frequency $\omega = 2\pi\nu$, namely,

$$W_{r\varphi} = -2\eta H R \frac{d\omega}{dR}, \tag{2}$$

where H is a half-thickness of a disk and η is turbulent viscosity. The nondimensional parameter that is essential for equation (??) is a parameter γ (often called the Reynolds number) which is the inverse of the SS73 α parameter for the accretion flow,

$$\gamma = \dot{M}/4\pi\eta H = RV_r/D, \tag{3}$$

where V_r is a characteristic velocity, and D is the diffusion coefficient. D can be defined as $D = V_t l_t/3$ using the turbulent velocity and the related turbulent scale, respectively or as $D = D_M = c^2/\sigma$ for the magnetic case where σ is the conductivity (e.g. see details of the D-definition in Lang 1998). We present $\omega(R)$ in terms of dimensionless variables, namely , angular velocity $\theta = \omega/\omega_0$, radius $r = R/R_0$ ($R_0 = x_0 R_S$, and $R_S = 2GM/c^2$ is the Schwarzchild radius) and mass $m = M/M_\odot$. We express the Keplerian angular velocity as

$$\theta_K = 6/(a_K r^{3/2}), \tag{4}$$

where $a_K = m(x_0/3)(\nu_0/363\ \mathrm{Hz})$; the rotational frequency ν_0 has a particular value for each star. Equations $\theta = 1$ at $r = r_{in}$ (the inner disk radius), $\theta = \theta_K$ at $r = r_{out}$ (the radius where the transition layer adjusts to the Keplerian motion), and $d\theta/dr = d\theta_K/dr$ at $r = r_{out}$ were assumed by TLM98 to be the boundary conditions. Thus, the profile $\theta(r)$ and the outer radius of the transition layer are uniquely determined by the boundary conditions and the angular momentum equation (1-3) for a given value of γ parameter. The solution of equations (1-3) satisfying the above boundary conditions is equation (10) in TLM98 and the equation (see TLM98, Eq. 11)

$$3\theta_{out}/2 = D_1 \gamma r_{out}^{-\gamma} + 2(1 - D_1) r_{out}^{-2} \tag{5}$$

determines $r_{out} = R_{out}/R_0$ as a function of γ parameter, where $D_1 = (\theta_{out} - r_{out}^{-2})/(r_{out}^{-\gamma} - r_{out}^{-2})$. The adjustment of the Keplerian disk to the sub-Keplerian inner boundary creates conditions favorable for the formation of a hot plasma outflow at the outer boundary of the transition layer (TLM98), because the Keplerian motion (if it is followed by sub-Keplerian motion) must pass through the super-Keplerian centrifugal barrier region. For the observed range from 1 to 100 Hz and from 0.1 to 10 Hz for of the high and low QPO frequencies respectively (see Fig. 2) one can find using the TLM98 solution for m=10 that γ varies from 2 to 20 (a variation which is related to the mass accretion rate $\dot{M}$ (see Eq. 3).

It is worth noting that in the literature that $\alpha = \gamma^{-1}$ is treated as a constant and a free parameter independent of the mass accretion rate (or the spectral state), whereas we find

that the α varies from 0.5 to 0.05 with $\dot{M}$, i.e. α is a real strong function of $\dot{M}$. This α variation has many consequences for the accretion disk model as well as in the interpretation of data (see discussion in Titarchuk & Shrader 2002).

2.2. Magnetoacoustic oscillations in the disk transition layer

The TL model identifies the low frequency QPO as that associated with the viscous magnetoacoustic (MA) oscillation of the bounded TL; this mode is common to both BH's and NS's. The correlation of the MA frequency with the gravitational (Keplerian) frequency $\nu_{\rm K} = 2\pi\omega_{\rm K}$ were derived by TO99, Titarchuk, Bradshaw & Wood (2001) for NS and then it was generalized by TW02, for BH and WD. The MA frequency is derived as the eigenfrequency of the boundary-value problem resulting from a MHD treatment of the interaction of the disk with the magnetic field. The problem is solved for two limiting boundary conditions which encompass realistic possibilities. The solution yields a velocity identified as a mixture of the sound speed and the Alfvén velocity. The TBW treatment does not specify how the eigenfrequency is excited or damped. However, it makes clear that the QPO is a readily stimulated resonant frequency [see Titarchuk, Cui & Wood (2002) and Titarchuk (2002) for details of excitation of the eigenfrequencies].

A linear relation was derived between ν_{MA} and $\nu_{\rm K}$ (see Fig. 2 and TW02)

$$\nu_{MA} = C_{MA}\nu_{\rm K}. \tag{6}$$

where $C_{MA} = 2^{1/2}4\pi[(1+f\beta)/(1+\beta)]^{1/2}(H/r_{out})$ is a proportionality coefficient which is "universal" to the extent that β and H/R_{out} remain about the same from one source to the next. Here $\beta = P_g/P_B$ is the ratio of the gas pressure to the magnetic pressure and the coefficient $f = 1/32,\ 1/32\pi^2$ for stiff and free boundary conditions respectively and H is the half-width of the Keplerian part of the disk.

Identification of ν_{high}, ν_{low}, with $\nu_{\rm K}$, ν_{MA} respectively, leads TW02 to determination of $H/R_{out} = 1.5\times10^{-2}$ and $\beta = 10$ using the observed value of $C_{MA} = 0.08$.

In Figure 3 we present the inferred ν_{low} ($\nu_{low} = 0.08\nu_{high}$) as a function of γ. We derive this relation using equations (4) and (5) with the assumptions that $a_{\rm K} = m(\nu_0/363\ Hz) = 1$ and $m = M/M_\odot = 10$.

It is evident that the inferred ν_{high}, ν_{low} are inversely proportional to m because

$$\nu_{high} = \nu_{\rm K} \propto m^{-1} \tag{7}$$

and

$$\nu_{low} \sim V/L, \tag{8}$$

where L is the TL characteristic size is proportional to m.

We calculate the size of the TL, $r_{out} = R_{out}/R_S$ as a function of ν_{low} using relations (6), and $\nu_{high} = \nu_K$. Because the radius of interest, which in our case is the outer TL boundary radius R_{out}, is related to ν_K one can relate R_{out} to ν_{low} using formula (6). We present this function in Figure 4.

The spectral index–frequency correlation can be derived if we find a spectral index–TL optical depth correlation. Because γ is proportional to the mass accretion rate $\dot{M}$ and the optical depth τ_0 is also proportional to $\dot{M}$, we are lead to a correlation of ν_{low} and τ_0 and ultimately to the index–frequency correlation.

2.3. Spectral index-optical depth relation. Corona model

It is an worthwhile and interesting question to ask if there is a common mechanism in the energy release (heating) in coronae of the compact objects (neutron stars and black holes). It is known from X-ray observations of BHs and NSs the emission from the hot coronal plasma (source of the hard radiation) is a significant fraction of the bolometric radiation. Particularly in the low/hard state the hard radiation (Comptonization) is dominant [5]. In hard state spectra in BHs and NS show are both well fitted by power law spectra which is a signature of Compton upscattering of the soft disk photons. The BH hard state spectra are characterized by spectral indices $\alpha = 0.6 \pm 0.2$ (or photon indices $\Gamma = 1.6 \pm 0.2$) and the plasma temperature about 50-100 keV independently of the luminosity level. In this state thermal Comptonization is dominant.

In this paper we argue that the heating of corona (Compact cloud) can be determined by the gravitational energy release there.

TLM98 offered the TL model adjustment of the Keplerian accretion flow (disk) to the sub-Keplerian innner boundary condition which provides a compact corona for Comptonization upscattering of the illuminating accretion disk photons. The essential sub-Keplerian rotation of NS in LMXBs is a well established observational fact due to the direct measurements of NS spins (see a review by van der Klis 2000 for details). The direct BH spin measurements are still unavailable but if we use analogy with NS rotation we can assume that BH may also undergo sub-Keplerian rotation.

---

[5] As the energy release in the solar corona 1.4×10^{28}erg s^{-1} is only small fraction of the solar irradiance 3.8×10^{33} erg s^{-1}.

It is likely that this adjustment to sub-Keplerian flow is not smooth and that near the adjustment radius the strong or weak shocks can be formed. *For a given viscosity η the position of the adjustment is determined by the disk mass accretion only* (see Eqs. 3 and 5). The adjustment radius (shock) region can be treated as a potential wall at which the accreting matter releases its gravitational energy in a geometrically thin target. As a consequence of this the shock plasma temperature is much higher than that in the surrounding regions of the Keplerian disk. The shock region gets puffed up oscillating with frequencies close to $\nu_{\rm K}$ (Titarchuk 2003). Additional oscillations can appear (at least in NS case) because of the rotational configuration above the disk which is a magnetosphere in NS case (see details in TOK). The shock formation leads to the formation of the hot inner bounded region. The hard photons in the shocked region illuminate the surrounding material evaporating some part of the disk. It is obvious that the evaporated fraction depends on the mass accretion rate in the disk (see Chakrabarti & Titarchuk 1995, hereafter CT95). Some small fraction of the hard photons (at maximum 6 %) can be reflected by the cold parts of the disk (CT95 and see also Basko, Sunyaev & Titarchuk 1974).

Let us assume the column density of this region y_0 is a few grams or that the Thomson optical thickness τ_0 is a few (see SS73 for the thickness estimate of the innermost part of the disk). The rate of energy release at this region Q_{cor} is a few percent of the Eddington luminosity since the adjustment radius is located within 4-100 Schwarzschild radii (see Fig. 4). The heating of gas due to the gravitational energy release should be balanced by the photon emission. For high plasma temperature, Comptonization and free-free emission is the main cooling channel, and the heating of electrons is presumably due to the Coulomb collisions with protons (see Fig. 1 for the picture of disk corona).

Under such physical conditions the energy balance can be written as [see also Zeldovich & Shakura (1969), hereafter ZS69 and TLM98]

$$Q_{cor}/\tau_0 = C_{comp}\varepsilon(\tau)T_e/f(T_e) + C_{ff}T_e^{1/2}\rho, \tag{9}$$

where τ is the optical depth within the shock, $\varepsilon(\tau)$ is a distribution function for the radiative energy distribution, $f(T_e) = 1 + 2.5(kT_e/mc^2)$ is the relativistic correction factor, T_e is the electron temperature in K, $C_{comp} = 20.2$ cm s^{-1} K^{-1} and $C_{ff} = 2.6 \times 10^{20}$ erg K$^{-1/2}$cm s^{-1} are a dimensional constants. In this formula we neglect the gas heating due to recoil effect.

The distribution $\varepsilon(\tau)$ is obtained from the solution of the diffusion equation (ZS69),

$$d^2\varepsilon/d\tau^2 = -3(Q_{tot}/c)/\tau_0 \tag{10}$$

subject to two boundary conditions. Here we assume that the region of the gravitational energy release (corona) is a spherical shell surrounding the central object and the total

flux in the corona is a sum $Q_{tot} = Q_{cor} + Q_d$ of the gravitational energy release Q_{cor} and the illumination flux from outside of the corona (disk) Q_d. The inner and outer boundary conditions for a BH corona are that there are no scattered radiation from outside of the corona. Then in the Eddington approximation (see Sobolev 1975) the boundary conditions can be written as follows :

$$(d\varepsilon/d\tau - 3\varepsilon/2)|_{\tau=0} = (d\varepsilon/d\tau + 3\varepsilon/2)|_{\tau=\tau_0} = 0, \tag{11}$$

where $\tau = 0$ and $\tau = \tau_0$ are at the inner and outer boundaries respectively.

For a NS corona one should assume that inside of the inner corona boundary the energy density ε =constant, namely that the radiation flux emitted towards the central object at some point of the inner boundary returns back (reflected by the NS surface), namely this condition is equivalent to the reflection condition:

$$d\varepsilon/d\tau|_{\tau=0} = 0. \tag{12}$$

Below we present a general formula of the coronal temperature which combines the BH and NS cases.

The solution of equations (10-11) provides us with the distribution function for the energy density in the BH corona

$$\varepsilon(\tau) = (Q_{tot}/c)\{1 + (3/2)\tau_0[\tau/\tau_0 - (\tau/\tau_0)^2]\}. \tag{13}$$

We neglect the dependence of Q_{tot} on τ to derive this formula. Furthermore, we take a representative value of $< \varepsilon >$ for the maximum value in the corona which is very close to mean value of ε_{mean} i.e.

$$< \varepsilon >= \varepsilon_{max} = (Q_{tot}/c)[1 + (3/8)\tau_0]. \tag{14}$$

in order to approximate the coronal temperature. In Figure 5 we present the results of calculations of the temperatures kT_e (keV) and the energy spectral indices of the Comptonization spectrum α (photon index $\Gamma = \alpha + 1$) as a function of the optical depth of the shell τ_0. The different curves of $T_e(\tau_0)$ are related to the different ratios of Q_d/Q_{cor}. The calculations have been made for values of $\rho = 10^{-6}$ g cm^{-3} and $Q_{cor} = 10^{22}$ erg cm^{-2} s^{-1} which are characteristic values of the density and luminosity for the standard disk model (SS73).

In fact, the calculation results weakly depend on ρ and Q_{cor} if

$$(\rho/10^{-6}\mathrm{g\ cm^{-3}})/(\mathrm{Q_{cor}}/10^{22}\mathrm{erg\ cm^{-2}s^{-1}}) \lesssim 1$$

is of order a few or less.

In this case the equation for the temperature is simplified

$$6.73 \times 10^{-2} \tau_0 (1 + 3\tau_0/8)(T_e/10^8\ K)(1 + Q_d/Q_{cor})/f(T_e) = 1 \quad (15)$$

which has the solution

$$T_e/10^8\ K = 1.5 \times [\tau_0(1 + 3\tau_0/8)(1 + Q_d/Q_{cor}) - 0.62]^{-1}. \quad (16)$$

It is easy to show that the case for which $Q_d/Q_{cor} = 1$ is identical to the NS case (the inner reflective boundary) when the disk illumination is neglected. One can see from Eq. (16) that T_e is a function of τ_0 if $Q_d/Q_{cor} \ll 1$. It is also worth noting that $T_e\tau_0(1 + 3\tau_0/8)/f(T_e)$ is insensitive to the total luminosity Q_{tot} if if $Q_d/Q_{cor} \ll 1$ (Eq. 15).

The spectral index α as a function of the product of $T_e\tau_0$ are insensitive to Q_{tot} too for $\tau \lesssim 1$ because the the Comptonization parameter

$$y = 4kT_e/m_ec^2\ \mathrm{Max}(\tau_0, \tau_0^2)$$

and

$$\alpha = -3/2 + \sqrt{(9/4 + 4/y)}$$

(see Rybicki & Lightman 1979 and Sunyaev & Titarchuk 1980). This inferred property of the Comptonization spectra reproduces the observed independence of α on the bolometric luminosity (see e.g. Tanaka 1995) when α varies within the range 0.6 ± 0.2 ($\Gamma = 1.6 \pm 0.2$). This defines the so called the low/hard state in BHs.

Below we show that the observed plateau of the index-frequency correlation at low values of $\nu_L < 1$ Hz is the result of this behaviour because the lower frequency values are related to the low mass accretion rates $\dot{m} = \dot{M}/M_{Edd} < 1$ and τ_0 is of order one when $\dot{m} < 1$.

We calculate the exact values of the spectral indices α for a given T_e and τ_0 using the relativistic formulas developed by Titarchuk & Lybarskij (1995) [see formulas (17), (for plane geometry, note their τ_0 is our $\tau_0/2$) and (24) there]. In Figure 5 we present the spectral indices as a function of τ_0 for BH and NS cases when the disk illumination is negligible small with respect to the coronal energy release (a condition which can be a model for the low/hard state in these systems). The plasma temperature values of 20-150 keV for $\tau_0 = 1 - 3$ and $\alpha = 0.6 \pm 0.2$ (for $ratio = Q_d/Q_{cor} = 0$) are typical values of these quantities for low/hard state in BHs.

When Q_d is comparable with Q_{cor} the cooling becomes more efficient due to Comptonization and free-free processes and therefore T_e unavoidably decreases [see T_e-values for $Q_d/Q_{cor} = (1 - 4)$ in Fig. 5].

This illumination effect and mass accretion rate increase may explain the hard-soft transition when the Compton temperature drops substantially with increase of the soft (disk) photon flux (for illustration, see Figure 1). In Figure 5 we show that temperature drops from 50-60 keV for $ratio = 0$ to 7-10 keV for $ratio = 4$. The temperature may drop also due to an increase in the optical depth (presumably because $\dot{m}$ increases) even when $ratio = 0$.

2.4. Modeling of spectral phase transition from the hard state to the soft state

Laurent and Titarchuk (1999), hereafter LT99, studied the Comptonization of the soft radiation in the converging inflow (CI) into a black hole using Monte Carlo simulations. The full relativistic treatment has been implemented to reproduce the spectra. An accreting black hole is, by definition, characterized by its drain effect , namely, matter falls into a black hole much the same way as water disappears down a drain: matter goes in and nothing comes out. The effect of the drain within the TL corona, i.e. the converging inflow, on the X-ray spectrum provides a unique observational signature of black holes. LT99 show that spectrum of the soft state of BHs can be described as the sum of a thermal (disk) component and the convolution of some fraction of this component with the CI upscattering spread (Green's) function. The latter boosted photon component is seen as an extended power law at energies much higher than the characteristic energy of the soft photons. LT99 demonstrate the stability of the power law index (the photon index, $\Gamma = 2.8 \pm 0.1$) over a wide range of the plasma temperature 0-10 keV, and mass accretion rates (higher than 2 in Eddington units) due to upscattering and photon trapping in the converging inflow. The spectrum is practically the same as that produced by standard thermal Comptonization (see e.g. Titarchuk 1994, Hua & Titarchuk 1995) when the CI plasma temperature is of order 50 keV (the typical ones for the BH hard state). In this case one can see the effect of the bulk motion only at high energies, where there is an excess in the spectrum with respect to the thermal Comptonization spectrum.

LT99 also demonstrate that the change of the spectral shapes from the soft state to the hard state is clearly related to the temperature and optical depth of the bulk inflow. We combine our results of calculations of index and Compton cloud temperatures for thermal Comptonization case (see §2.3 and Fig.5) and LT99's results of the spectral calculations (see Table 2 in LT99 for the spectral index values) to evaluate the power law index as a function of the optical depth of the Compton cloud τ_0. We use the values of the index and of the temperature for $Q = 0$ (see Fig. 5) when τ_0 varies from 1 to 3 to decribe the index behavior and the plasma temperature variation in the hard state. Figure 6 presents the photon index

Γ as a function of τ_0. This function $\Gamma(\tau_0)$ can be fitted analytically as follows:

$$\Gamma(\tau_0) = c_0 + c_1\tau_0 + c_2\tau_0^2 + c_3\tau_0^3 \quad \text{for} \quad 1 < \tau_0 \leq 5.17,$$
$$\Gamma(\tau_0) = b_0 - b_1 e^{-\tau_0/\tau_*} \quad \text{for} \quad \tau_0 > 5.17 \tag{17}$$

where $c_0 = 0.61$, $c_1 = 0.57$, $c_2 = 1.485 \times 10^{-2}$, $c_3 = -8.5 \times 10^{-3}$ and $b_0 = 2.81$, $b_1 = 1.0 \times 10^3$ and $\tau_* = 0.5$.

In order to derive the index dependence Γ on ν_{low} one should relate the parameter γ to τ_0 and then combine the two relationships Γ vs τ_0 and ν_{low} vs γ (see Figures 3-6). In the first approximation τ_0 should be proportional to γ because both of them are proportional $\dot{M}$. To fit the data we assume that $\tau_0 = A\gamma^\delta$. We have three free parameters, black mass $m = M/M_\odot$, δ and A to fit the model to the data if we assume that the converging inflow (CI) is essentially cold (the CI temperature $kT_{ci} < 5$ keV).

3. Data and Analysis

We analyze data points for photon index vs low frequency correlation obtained from Trudolyubov et al. (1999) and Vignarca et al. (2003) for GRS 1915+105 and Sobczak et al. (1999, 2000) for XTE J1550-564. Also we make use data for GRS 1915+105 by Fiorito, Markwardt & Swank (2003) hereafter FMS, which is a detailed study of QPO and spectral features of the steady low hard states of GRS 1915+105 for representative 1996 and 1997 observations. FMS computed the power spectra of combined Binned and Event Mode data for PCA channels 0-255 and sampled at 0.25-64 Hz for 4-second intervals. The spectra were averaged over the entire observation duration. The PDS spectra were fit with a combination of Lorentzian lines and exhibited a break frequency, a central QPO frequency and in some case the presence of the first harmonic. Background subtracted energy of each OBSID were obtained and time average over the entire observation duration using Standard 2 PCA and HEXTE data where available (both clusters). The XSPEC model used to fit the energy spectra consisted of a multi-temperature thermal disk component (DISKBB), a simple power law and a small Iron line component. For the 1996 data (OBSID10408), it was found that the disk component could be neglected without affecting the fit. Acceptable χ^2 were obtained in all cases.

3.1. Correlations between QPO Frequency and Spectral Parameters

The first part of the FMS study was to first to look for correlations of different spectral components, presumably thermal disk components, with QPO frequency to try to determine

the reason for the non-unique total flux correlations previously observed. In the case of OBSID 20402 (1997) we did observe the expected positive correlation of QPO frequency with disk flux in agreement with previous analyses of Muno et al. (1999) and Markwardt et al. (1999), which were done in other states. However, we observed an anti-correlation of frequency with disk flux for OBSID 10408 (1996); and no correlation of frequency with disk flux for OBSID 10258 (1996). Furthermore, no correlation of QPO frequency with disk temperature is seen for any of the OBSIDS we studied. These results are at variance with the often-quoted result that disk parameters are closely associated with QPO frequency. Remillard, et. al. (2002) show a comparison of low QPO frequency and the apparent disk flux for the source XTE J1550-564 during its 1998-1999 outburst. The QPOs are reported with differences in phase lags. Again, it is clear that a frequency-disk flux correlation is observed for this source is only observed at lower ($\nu < 5$ Hz) QPO frequencies and fluxes than usually observed for GRS 1915+105.

However, robust correlation between index and the central frequency of low frequency QPOs are also seen in a wide variety of BH sources radiating in different states and during transition between states. The QPO frequencies in such studies are observed in the PDS obtained by integrating over time intervals ranging from the complete time of the observation to segmented time bins where the luminosity remains constant, [see e.g. Markwardt, et. al (1999)]. Strong frequency-index correlations are observed by Kalemci (2002) in outburst decay (presumably state transitions) of a number of sources and by Vignarca, et. al. (2003), in a comprehensive study which focuses its attention on the behavior of the power law index and QPO frequency in several BH candidate sources. We will use the data of Vignarca, our studies and that of other as well in our analysis (see §3.2 below).

Observation of low term tracking of the QPO frequency with the variations of the photon index has been observed in at least two BH sources. Tracking is seen in the data of Rossi (2003) and Homan (2001) in observations of XTE J1560-500 taken over a 30-day period. In this period the source apparently transits from the low hard state ($\Gamma \sim 1.5$) to the intermediate or soft state where the index apparently remain close to the constant at a value ($\Gamma \sim 2.5$). In this transition the QPO frequency varies from about 1 to 10 Hz. Similar tracking is observed in XTE J1550-564 by Sobzcak et al. (1999), (2000). However, the index and QPO frequency does not track with the total X-ray flux (Vignarca et al. 2003, Figure 7).

3.2. Comparison of the inferred index-frequency correlation with the data

3.2.1. Low/Hard-High/Soft State Transitions

GRS1915+105

In Figure 7 we present the results of fit to the data of Vignarca, et. al (2003) for the plateau observations of the microquasar GRS 1915+105 using the TL model. The best fit parameters are $m = 12$, $\delta = 1.25$ and $A = 1$. We note that the value $m = 12$ is consistent with the BH mass evaluation $m = 13.3 \pm 4$ obtained by Greiner et al. (2001) using the IR spectra and by Shrader and Titarchuk (2003) (see also Borozdin et al. 1999) using the X-ray spectra. The observable index saturations at low and high values of ν_L are nicely reproduced by the model. The low and high frequency plateau regions of the data and fit are signatures of the two spectral phases which are explained by two different regimes of Comptonization (upscattering): (1) bulk flow Comptonization in the soft state (saturation at $\Gamma \sim 2.8$) and (2) thermal Comptonization in the hard state (the photon index tends to level at $\Gamma \sim 1.5$).

A comparison of the index-frequency correlation of plateau observations with Vignarca's β and ν data [Belloni (1999) classification scheme] and the model fits are plotted in Figure 8. The only difference in the data is different saturation values at high ν_L that can be readily explained by a change of plasma temperature in the converging inflow kT_{ci}. For upper value of $\Gamma = 2.81$ the temperature $kT_{ci} = 5$ keV as for $\Gamma = 2.7$ the temperature $kT_{ci} = 9$ keV. The best-fit parameters for the latter data are the same as for the plateau observations except that in the model function $\Gamma(\tau_0)$ (see Eq. 17) the coefficents b_0, b_1 and $\tau_\star$ are replaced by $b_0 = 2.7$, $b_1 = 22.4$ and $\tau_\star = 0.8$ for $\tau_0 > 2.47$.

In Figure 9 we present a plot of power-law index versus QPO centroid frequency for the observations of class α and ν of GRS 1915+105 from Vignarca et al. (2003) (black points=obs. 18). Blue points correspond to the values for observations by Fiorito et al (2003) for OBSID 20402 and OBSID 10258. Magenta points correspond to positions where the OBSID 20402 data points are shifted to one half the measured QPO low frequency values. This suggests that the latter data points are related to the second harmonics of the ν_L frequencies. It is well known that data for NS QPOs is a mixture of the first and the second harmonics of horizontal branch oscillation (HBO) frequencies (see e.g. van der Klis 2000). Red points correspond to positions where should be points with half of frequencies for Vignarca' s obs. 18. A theoretical curve (blue solid line) obtained using $\Gamma(\tau_0)$ (see Eq. 17) (for coefficents $b_0 = 2.7$, $b_1 = 22.4$ and $\tau_\star = 0.8$ for $\tau_0 > 2.47$) for $m = 12$ and $\tau_0 = \gamma^{1.5}$) fits the Fiorito's OBSID 10258 data points.

It is worth noting that relation between γ and τ_0 is slightly different from that we obtained for the best-fits presented in Fig. 8. Namely, the index of γ, increases from 1.25 to

1.5. It means that for the same value of γ the optical depth τ_0 is slightly higher than that in state presented in Fig. 8. This change can be explained by the slightly higher plasma accummulation in the transition layer.

It is interesting that the suggested half-frequency points (magenta and red ones) are located in a narrow corridor between these inferred curves (presented in Fig. 8 and Fig. 9 respectively).

XTE J1550-564

Figure 10 shows a plot of power law index versus QPO frequency for XTE J1550-564 from Vignarca et al. The data again shows a flattening out or saturation of the index at a value $\Gamma \sim 2.8$. It is clearly seen from Fig. 8 of Vignarca et al. that most of the points presented there can be fitted by the smooth line but a few points on the right that we exclude for a consideration for a while. The shift transformation $\nu'_L = 12\nu_L/10$ of the GRS 1915+105 curve, $\Gamma(\nu)$ (see Fig. 7) into $\Gamma(\nu')$ produces a fit for the XTE 1550-564 data. This means that if two sources in the same accretion regime [i.e. when $\tau_0(\gamma)$ is the same] their relative BH masses can measured by the simple shift transformation $\nu'_L = m_1\nu_L/m_2$. In our case we use $m_1 = 12$ for GRS 1915+105 and $m = 10$ for XTE 1550-564. These values are very close to the values that have been obtained by Shrader & Titarchuk (2003) for these sources using X-ray spectroscopic methods (Shrader & Titarchuk 1999). Thus the TL model provides an independent way to estimate the mass of one or more BH's in the same accretion state.

Comparison of all data points of the correlation of photon index vs QPO low frequency for XTE 1550-564 (black points) with the inferred correlation is shown in Figure 11. The saturation index value in the theoretical curve is related specific value of the plasma temperature of the converging inflow kT_{ci}, which changes from 5 keV to 20 kev from the top curve to the bottom respectively. Slightly different cooling regimes of the site of the converging bulk inflow can explain the different saturation levels of the index observed in XTE 1550-564. The temperature of the converging inflow is determined by the disk illumination geometry and by the intrinsic heating of the flow by pairs produced very close to horizon (see Laurent & Titarchuk 2004). All these effects may be manifested by the observed index-frequency correlation at high values of ν_L.

4U 1630-47

Figure 12 shows a plot of index versus QPO frequency for 4U 1630-47 [Tomsick & Kaaret (2000), Kalemci 2002). The data again show a similar behavior to that of XTE J1550-564 with an index saturation at $\Gamma = 2.45$ and $\Gamma = 2.7$. One can sees two phases with the index level at $\Gamma = 1.7 \pm 0.1$ and $\Gamma = 2.6 \pm 0.1$ and the transition between them that is much sharper than that observed in the other sources . The best-fit curve $\Gamma(\nu_L)$ (solid line) is obtained using $\tau_0 = 1.6\gamma^{0.36}$ and $\Gamma(\tau)$ function (see formula 17) for the best-fit BH mass $m = 16$

which is close to the estimate made by Borozdin et al. (1999) using the X-ray spectroscopic method. The dash curve is for saturation index value $\Gamma = 2.45$ (related to $kT_{ci} = 20$ keV). In this case $b_0 = 2.45$, $b_1 = 53.7$ and $\tau_* = 0.55$ for $\tau_0 > 2.2$). Our explanation for the observed anomalously sharp transition is as follows. A sharp phase transition may occur in a source where a thick disk is formed which penetrates the coronal region as the mass accretion rate increases (the underlying disk is probably evaporated by corona at small mass accretion rates). The cool thick disk then provides an additional source for coronal cooling in addition to the the external disk illumination of the corona. The corona gets cold faster and the bulk motion Comptonization becomes a dominant process in the upscattering of soft disk photons for that $\Gamma = 2.5 - 2.9$.

3.2.2. Very High/Soft or Extended Power Law States

GRS1915+105

As mentioned above observations in the "χ " states of GRS1915 by Vignarca et al. show a monotonically increasing linear correlation of frequency with index over a decade increase in QPO frequency. In this respect these results are similar to the observations of Kalemci (2002). What is particular interesting about Vignarca's GRS1915 data is that it completely complements the data presented by Kalemci, and shows that GRS1915+105 is quite similar to many other BH candidate sources with respect to the range of indices and QPO frequencies observed . FMS have also studied the behavior of the power index with QPO frequency in other plateau "χ" states of the microquasar GRS1915+105. Like, Vignarca, et. al., they have employed, a simple power law and thermal disk component as the primary constituents of the spectral model used to fit the spectra. FMS show the correlations observed in the three "χ" states, as mentioned above. The difference between the FMS results and those obtained by Vignarca et al. is that the former's data extends the range of indices and QPO frequencies to higher values observed in the data analyzed by Vignarca et. al. In the substates observed by FMS, the positive correlation of frequency and index for some OBSID's appears to be unbounded, i.e. there is no indication of saturation of the index value. Also the correlations observed by FMS for each of the OBSID's is different, i.e. the data does not fall on one line as is apparently the case for the Vignarca data, but falls on separate lines two of which appear to have the same slope.

It is interesting to compare the extended power law index ($\Gamma > 3$) results mentioned above with those of Rau and Greiner (2003), hereafter RG. who also observe a strong position correlation between photon index and power law normalization observed in "χ" states of GRS 1915+105. They have found that their data fall on two distinct positive correlation curves

as shown in their Figure 5. Their data (like FMS) shows an extended region of index values well beyond the saturation values observed in the soft state , i.e. $\Gamma \approx 2.8$ up to values as high as $\Gamma = 3.5$. This very high/soft (thermal) state is also observed in the data of Vignarca, et. al. for the source XTE J1748-288, where all the observed indices range from $\Gamma = 2.7 - 3$ and increase monotonically with QPO low frequency. This is the same type of behavior observed in the extended power law data of GRS1915+105 mentioned above.

We offer the following possible explanation for this data. The very high indices observed are due to a softening of the entire spectrum due to downscattering of escaping upscattered photons emerging from the central Comptonizing region by an extended cloud or outflowing wind of cold electrons well outside the TL region. This leads to an unbounded softening of the power law component. This type of spectral behavior has been characterized by Falcke (2003) as a possible jet dominated spectral state, referring to Comptonization of disk photons off a strong outflow of matter surrounding the BH.

RG have also compared the relationship between radio flux and X-ray power law index. RG observe a positive correlation between the X-ray photon index and the radio flux, a negative correlation between X-ray flux and radio flux for hard X-ray photons (E > 20 keV) and no correlation between X-ray flux and radio flux for 1-200 keV X-rays. In terms of our model the observed correlation is expected for the high energy photons but not for the bulk photon flux in the 1-200 keV energy band which is mostly determined by the low energy disk photons. On the other hand the soft photons are less affected by downscattering and thus one does not expect correlation of the jet power (outflow rate) with 1-200 keV photon flux. Thus the radio data is in agreement with our model.

3.3. Turnover States

GRO J1655-40

Vignarca's Figure 6 plots the index–frequency for two sources XTE J1550-564 and GRO J1655-40 together. The behavior of the later sources is quite distinct from all others analyzed - it shows a reverse or *negative* correlation between photon index and frequency. This is the only case known to exhibit this type of behavior. It is also noted that the two data sets appears to complement one another even though they occur in separate sources. Such a complementarity though with different slope has been noted above between XTE J1748-288 and XTE J1550-564. It is worth noting that the saturation plateau and turnover occur at indices lower than 2.8-2.9. This turnover and plateau behavior can be explained in terms of our model either by inefficient cooling of the converging flow by the soft disk photons or by heating of the converging flow corona by emergent pairs generating near the BH horizon

(see Laurent & Titarchuk 2004 for details). Indeed, at high mass accretion the outflow pairs are quenched by the accreted electrons and the pairs deposit their energy in the flow. The increase of the converging flow plasma temperature leads to more efficient upscattering and thus to lower values of index (LT99).

3.4. Correlations between High and Low Frequency QPO's

Strong correlations between high and low frequency QPO's in cases where both can be simultaneously observed (see e.g. Swank 2001 for GRS1915+105 and Homan 2001 for XTE J1550-564). This type of correlations indicates the presence of nonlinear resonances which are expected in the inner most region near the BH. It is evidence that the region of origin of the QPOs is indeed very close to the BH as the TL model predicts.

In Figure 2 we present data points showing low-high frequency dependence from BPK (see also PBK), Mauche (2002) and Woudt & Warner (2002) along with a fitted line $\nu_{low} = 0.081\nu_{high}$. The plot combines data points for BH, NS and white dwarf (WD) systems. A reader can find the details of these observations and the QPO data analysis in BPK, PBK and Mauche (2002). Each data point is strickly observational, representing two QPO frequencies that are detected at the same time in some particular source. TW02 interpreted this observational correlation and identification of ν_{high}, ν_{low} with $\nu_{\rm K}$ and ν_{MA} respectively, lead them to determination $H/R_{out} = 1.5 \times 10^{-2}$ and $\beta = 10$ (where H is the half-width of the disk and β is a ratio of the gas pressure to the magnetic pressure).

4. Summary and Conclusions

We have developed a model of accretion onto a Black Hole which greatly simplifies and reclassifies the plethora of "states" observational assigned to categorize the X-ray observations of variable BHC into two generic phases (states):

I) *soft state* where we see the effect of the BH as a "drain". Bulk inflow upscattering and its quenching effect on the Comptonization of disk photons dominates the behavior of the BH spectrum. The power law spectrum is steep in this situation. The observed high energy photons are emitted from a compact region, where soft energy photons of the disk are upscattered by bulk matter inflow forming the steep power law with photon index around 2.8, and low QPO frequencies (above 10 Hz) and high QPO frequencies (of the order of 100 Hz) are observed. In terms of the relativistic particle acceleration in the region of the corona and its effect on upscattering the soft disk photons, the soft state spectrum is a result of the

first order Fermi acceleration with respect to V/c.

We would like to emphasize that bulk inflow is present in BH when the high mass accretion is high *but not in NS*, where the presence of the firm surface leads to the high radiation pressure which eventually stops the accretion. The bulk inflow and all its spectral features are absent in NSs, in particular, the saturation of the index $\Gamma \sim 2.8$ with respect to QPO frequency, which is directly related to the optical depth and mass accretion rate, observed in the soft spectral state of only BHs and is therefore a particular signature of a BH.

II) *hard state,* which is comparatively starved for accretion. The hard phase (state) is related to an extended thermal Compton scattering cloud (cavity) characterized by a photon index $\Gamma \sim 1.5$ and the presence of low QPO frequencies (below 1 Hz). The low-hard spectrum is a result of the Fermi acceleration of the second order with respect to $(V/c)^2$. The effect of the first order on V/c is smeared out by the quasi-symmetry of the particular dynamic, predominantly thermal motion of the Compton cloud plasma.

The Transition Layer Componization Model: i. specifies the precise behavior of the power law index for each state; ii. identifies the origin and nature of low frequency and high frequency QPOs; iii. predicts and explains the observed relationship between them and their dependence mass accretion rate and spectral photon index for each of the phases; iv. predicts and explains the observed robust correlation of low frequency QPOs with spectral index observed in BHCs; v. predicts and explains the observed correlation between low and high frequency QPOs in BHs, neutron stars and white dwarfs. We interpret the correlation between low frequency ν_{low} and power-law photon index Γ in quasi-periodic oscillations (QPO) extensively investigated by Vignarca et al. (2003) and Kalemci (2002) for a variety of BH sources and states and also by Homan et al. (2001) and FMS. The observed correlation strongly constrains theoretical models and provides clues to understanding the nature of the QPO phenomena particularly in BHs and in compact objects in general.

In particular: (1) We find that the observed low frequency - the index correlation is a natural consequence of an adjustment of the Keplerian disk flow to the innermost sub-Keplerian boundary conditions near the central object. This ultimately leads to the formation of the sub-Keplerian transition layer (TL) between the adjustment radius and the innermost boundary (the horizon for BH).

(2) In the framework of the TL model ν_{high} is related to the gravitational frequency at the outer (adjustment) radius $\nu_g \approx \nu_K$ and ν_{low} is related to the magnetoacoustic oscillation frequency ν_{MA}. Using a relation between ν_{MA} and the mass accretion rate and the photon index Γ and the mass accretion rate we infer a correlation between ν_{MA} and the spectral

index Γ.

(3) Identification of ν_{low} with ν_{MA}, allow us to make a comparison of the theoretically predicted correlation with the observed correlation. For this identification we use the one temperature plasma assumption. We apply the plasma temperature obtained from the Comptonization spectra (electron temperatures) for calculations of magnetoacoustic frequencies which strongly depends on the proton temperature. The one temperature assumption is really consistent with the data.

(4) We present strong arguments that in BHs the two particular distinct phases occur in which one of them, the steep power-law phase is a real BH signature.

(5) We found that a hard phase (state) related to an extended Compton cloud (cavity) characterized by the photon index around 1.5 and the low QPO frequencies below 1 Hz. This is the regime where thermal Comptonization dominates the upscattering of soft disk photons and the spectral shape (index) is almost independent of mass accretion rate.

(6) We find that the soft phase (state) is related to the very compact region where soft energy photons of the disk are up scattered forming the steep power law spectrum with photon index saturating around 2.8. This is the regime where bulk flow Comptonization dominates and the effect of an increase in the mass accretion is offset by the effect of photon trapping in the converging flow into the BH.

(7) A extended power law regime where strong outflows obscure the bulk in flow region can also be present when the cold outflow from winds downscatters the emerging high energy photons and soften the observed spectrum. A regime of high accretion rate can also exist in this state where pair production heating adds to and can dominate the heating in the cavity causing a transition back to thermal Comptonization phase. In this phase a reverse correlation between low QPO frequency can result and is our explanation of the single case where this phenomena is observed.

(8) In the context of distinction between NS and BH sources it is worth pointing to a certain situation that can occur in low hard states. The source should be a NS if the soft blackbody like component with the color temperature of order of keV is present in the spectrum (Torrejon et al. 2004). In contrary, such a high temperature is necessary related to the high disk luminosity in a BH case.

(9) We offer a new method of BH mass estimate using the index-frequency correlations. Namely, if the theoretical curve of the index-frequency dependence $\Gamma(\nu_L)$ related to the parameter m_1 fits the data for a given source then the simple slide of the frequency axis $\nu'_L = (m_1/m2)\nu_L$ with respect to ν_L may allow us to obtain the mass m_2 by fit of $\Gamma(\nu'_L)$ to

the observable correlation for another source.

We acknowledge Tomaso Belloni for kindly supplying us data shown in Figures 7-12.

REFERENCES

Basko, M.M., Sunyaev, R.A., & Titarchuk, L. , 1974, A&A, 31, 249

Belloni, T., 2003, astro-ph /0309028

Belloni, T., Psaltis, D., & van der Klis, M. 2002, ApJ, 572, 392 (BPK)

Belloni, T., et. al. 2000, A&A, 355, 271

Boirin, L., Barret, D., Olive, J.F., Bloser, P.F., & Grindlay, J.E. 2000, A&A, 361, 121

Borizdin,K., et. al. 1999, ApJ, 517, 367

Chakrabarti, S.N. & Titarchuk, L. 1995, ApJ, 455, 623 (CT95)

Ebisawa, K. , Titarchuk, L. and Chakrabarti, S. 1996, Publ. Astron. Soc. Jpn. 48, 59

Di Salvo, T., Mendez, M., van der Klis, M., Ford, E., & Robba, N.R. 2001, ApJ, 546, 1107

Falcke, H. 2003 , Proc. of the Supermassive, Intermediate Mass and Stellar Mass BH Conf., Kyoto, Japan (to be published)

Fiorito, R., Markwardt, C., Swank, J. 2003, HEAD03 (FMS)

Ford, E., & van der Klis, M. 1998, ApJ, 506, L39

Greiner, J., Cuby, J.-G., McCaughrean, M.J. 2001, Nature, 414, 522

Grove, J.E., 1998, ApJ, 500, 899

Homan, J., et al. 2001, ApJS, 132, 377

Kalemci, E., 2002, Thesis, UC San Diego (unpublished)

Lang, K. R., 1998, Astrophysical Formulae, (Berlin: Springer)

Laurent, P. & Titarchuk, L. 2004, in preparation

Laurent, P. & Titarchuk, L. 2001, ApJ, 562, L67 (LT01)

Laurent, P. & Titarchuk, L. 1999, ApJ, 511, 289 (LT99)

Markwardt, C. et al. 1999, ApJ, 513, L37

McClintock, J. and Remillard, R., 2003, astro-ph/0306213

Mauche, C. 2002, ApJ, 580, 428

Morgan, E.H., Remillard, R.A., & Greiner, J. 1997, ApJ, 482, 993

Nowak, M.A. 2000, MNRAS, 318, 361

Nowak, M.A., Wilms, J., & Dove, J.B. 2002, MNRAS, 332, 856

Psaltis, D., Belloni, T. & van der Klis, M. 1999, ApJ, 520, 262 (PBK)

Rau, A. and Greiner, J. 2003, A&A 397, 711 (RG)

Remillard, R. et al. 2002, astro-ph/0208402

Rossi, S. et al. 2003, astro-ph/0309129

Rybicki, G.B. and Lightman, A.P. 1979, Radiative Processes in Astrophysics, John Wiley & Sons

Shakura, N.I. & Sunyaev, R. A. 1973, A&A, 24, 337

Shrader,C. and Titarchuk, L. 1998, Ap J, 499, L31

Sobolev, 1975, Light Scattering in the Atmosphere, (Oxford: Bergamon)

Sobzcak, G.J., et al. 1999, ApJ, 517, L121

Sobzcak, G.J., et al. 2000, ApJ, 531, 537

Strohmayer, T.E., et al. 1996, ApJ, 469, L9

Swank, J. 2001, Astrophysics and Space Science (supl.), 276, 201

Sunyaev, R. & Titarchuk, L. 1980, A&A, 86, 121

Tanaka, Y. and Lewin, G.H., X-ray Binaries, (Eds. Lewin W.G.H., van Paridis, J. and van den Heuvel, E.P.J.), p 126, Cambridge Univ.

Titarchuk, L., 2003, ApJ, 591, 354

Titarchuk, L., Cui and Wood, K., 2002, ApJ, 576, L49

Titarchuk, L. and Lybarskij, Yu. 1995, ApJ, 450, 876

Titarchuk, L. and Shrader, C. 2002, ApJ, 567, 1057

Titarchuk, L. and Wood, K., 2002, ApJ, 577, L23 (TW02)

Titarchuk, L., Bradshaw, C. F., & Wood, K.S. 2001, ApJ, 560, L55 (TBW)

Titarchuk, L., Bradshaw, C. F., Geldzahler, B.J., & Fomalont, E.B. 2001, ApJ, 555, L45

Titarchuk, L. & Osherovich, V. 1999, ApJ, 518, L95 (TO99)

Titarchuk, L., Osherovich, V., & Kuznetsov, S., 1999, ApJ, 525, L129 (TOK)

Titarchuk, L., Lapidus, I.,& Muslimov, A. 1998, ApJ, 499, 315 (TLM98)

Titarchuk, L., Mastichiadis, A. and Kylafis N., 1997, ApJ, 487, 834

Titarchuk, L., Mastichiadis, A. and Kylafis N., 1996, Astron. Astrophys. Sup. 120, C171

Titarchuk, L. and Zannias, T. Ap J, 493, 863

Torrejon, J.M., et al. 2004, A&A, in press

Trudolyubov, S.P., Churazov, E.M. & Gilfanov, M.R. 1999, Astr. Lett., 25, 718

van der Klis, M. 2000, ARA&A, 38, 717

van der Klis, M., et al. 1985, Nature, 316, 225

Vignarca, et al. 2003 A&A, 397, 729 (V03)

Wijnands, A.D. & van der Klis, M. 1999, ApJ, 514, 939

Woudt, P.A., & Warner, B. 2002, MNRAS, in press, astro-ph/0202441

Zeldovich, Ya. B., & Shakura, N.I. 1969, Sov. Astron. 13,175

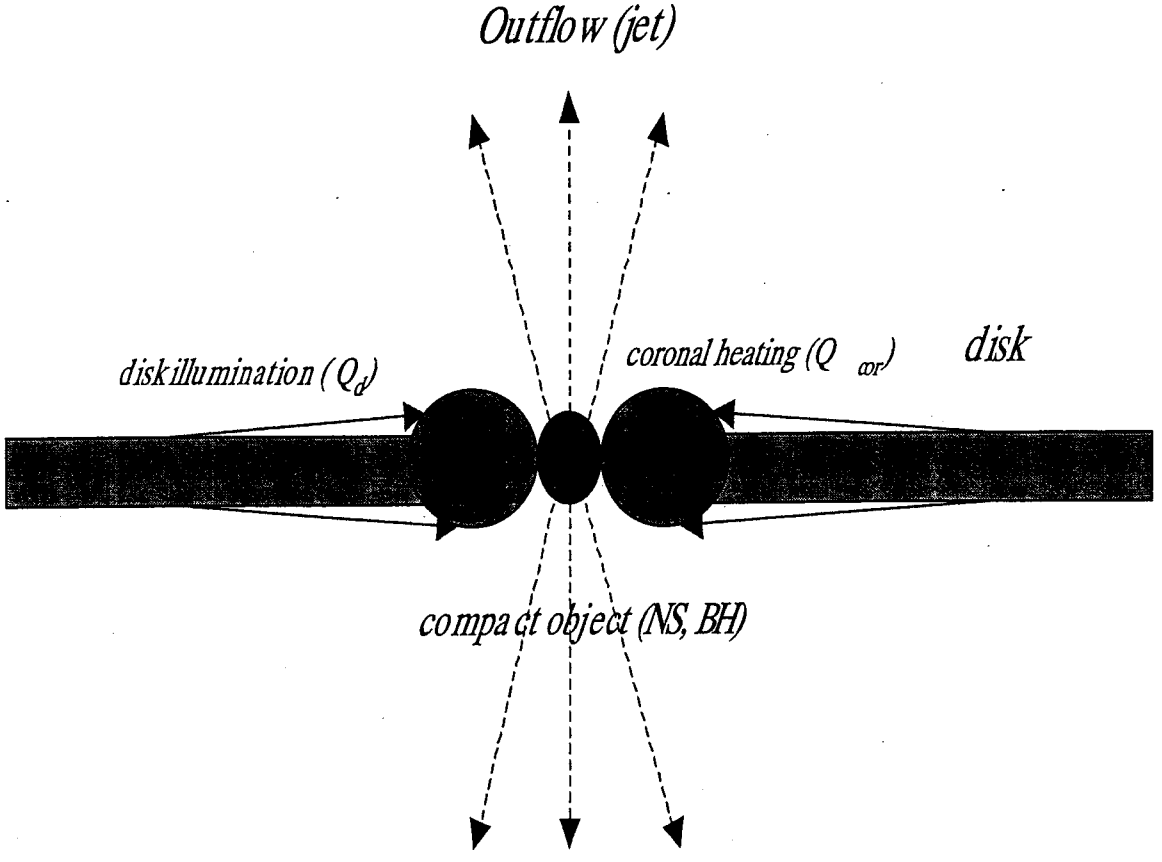

Fig. 1.— Transition layer (corona) concept. This picture renders the gravitional energy release in the disk and corona and the coronal illumination by the disk soft flux in compact object (NS and BH). See details in text

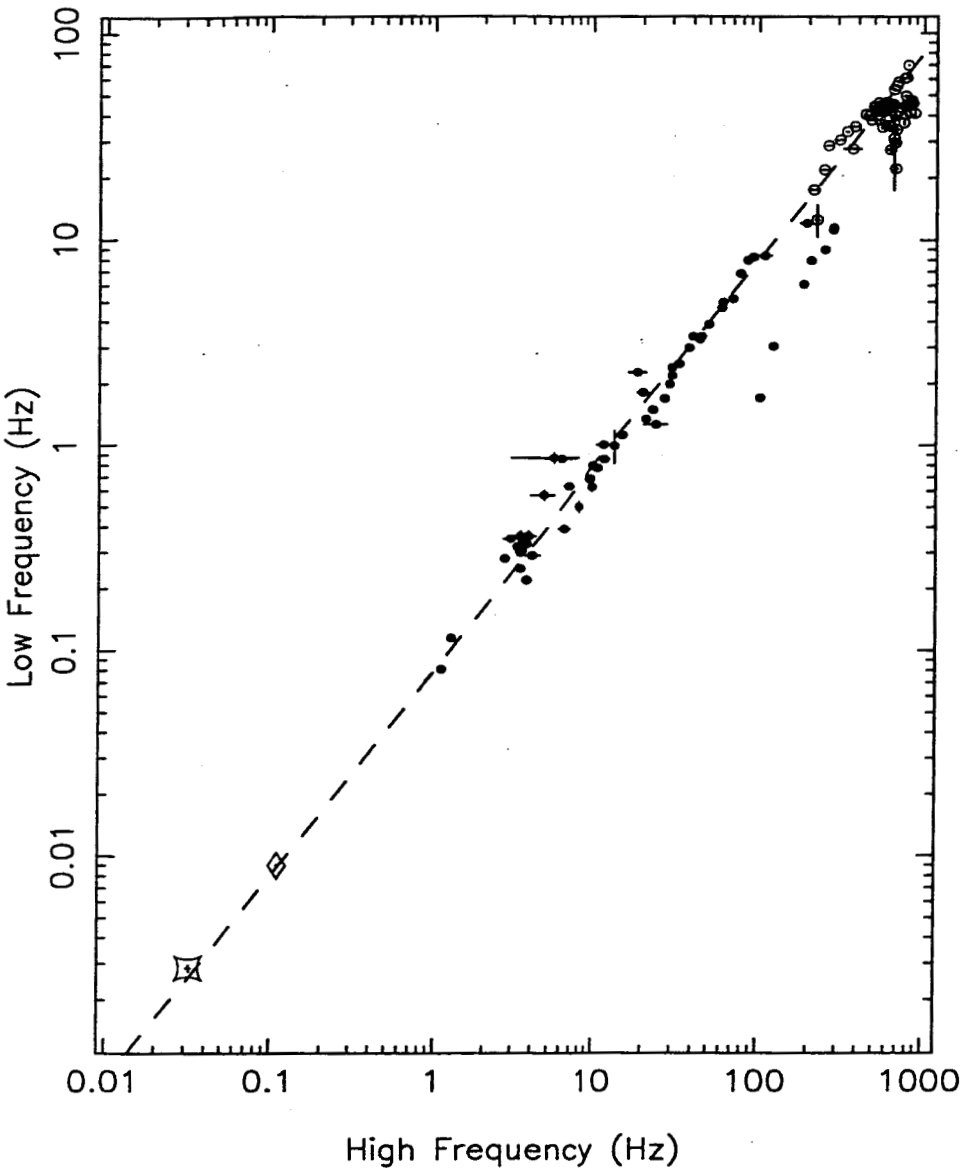

Fig. 2.— Correlation between frequencies of QPO and noise components white dwarfs [diamonds for SS Cyg (Mauche 2002); squares for VW Hyi (Woudt & Warner 2002)] , neutron star (open circles) and, black hole candidate (filled circles) sources. Neutron star and black hole data are from Belloni, Psaltis & van der Klis (2002). The dashed line represents the best-fit of the observed correlation (see TBW01 and TW02 where this correlation is predicted and explained using the TL model). This plot also appears in Mauche (2002).

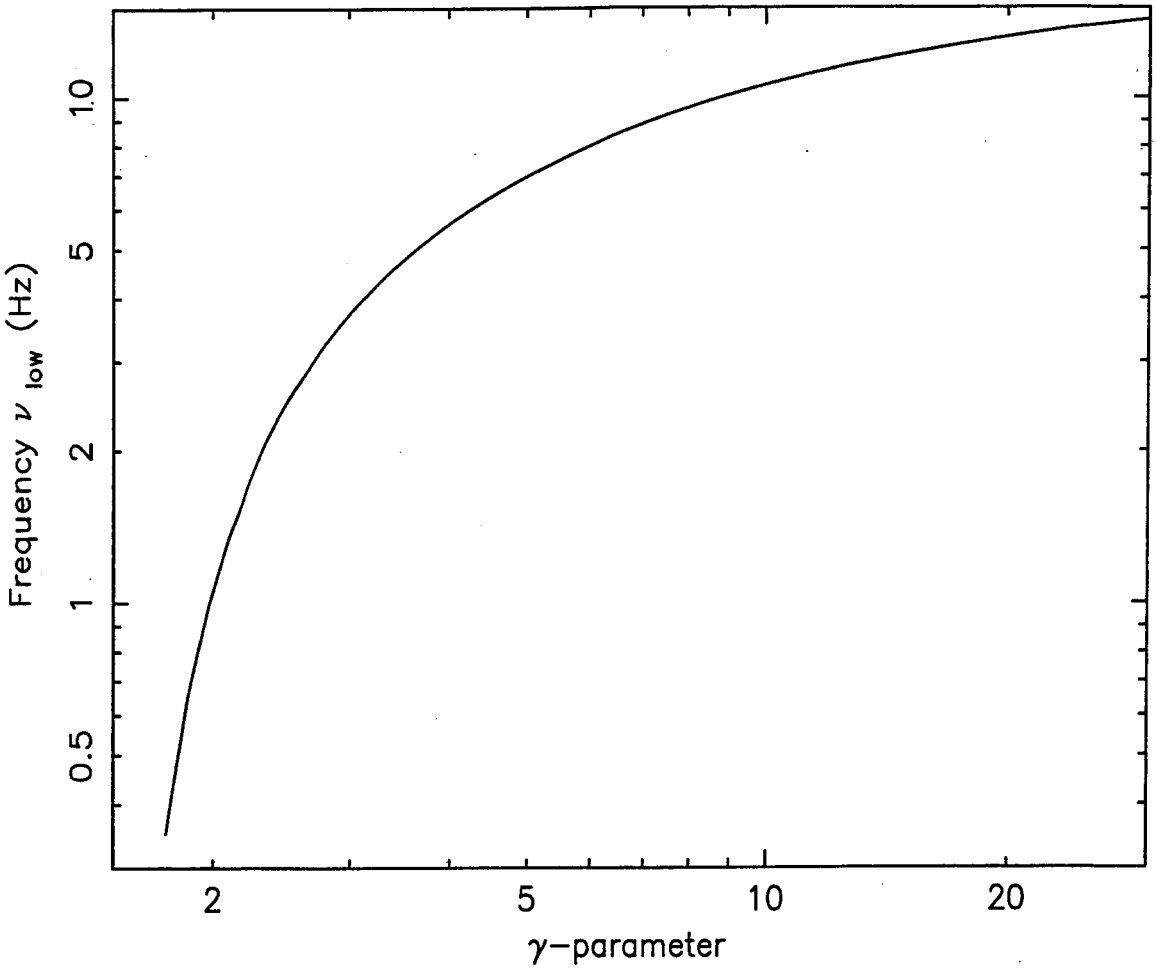

Fig. 3.— Plot of QPO low frequency vs. γ parameter ($\propto \dot{M}$).

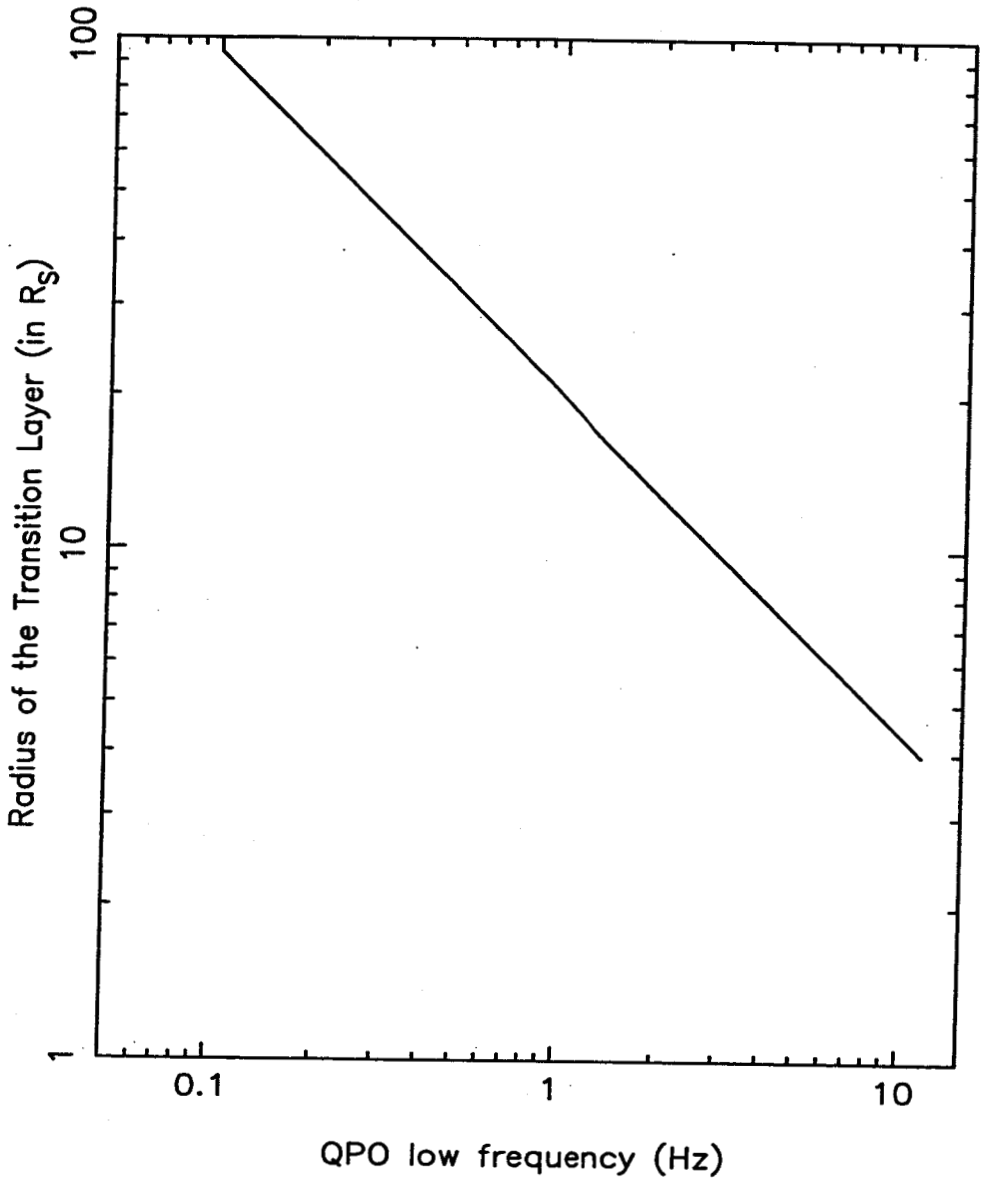

Fig. 4.— Radius of the transition layer vs QPO low frequency.

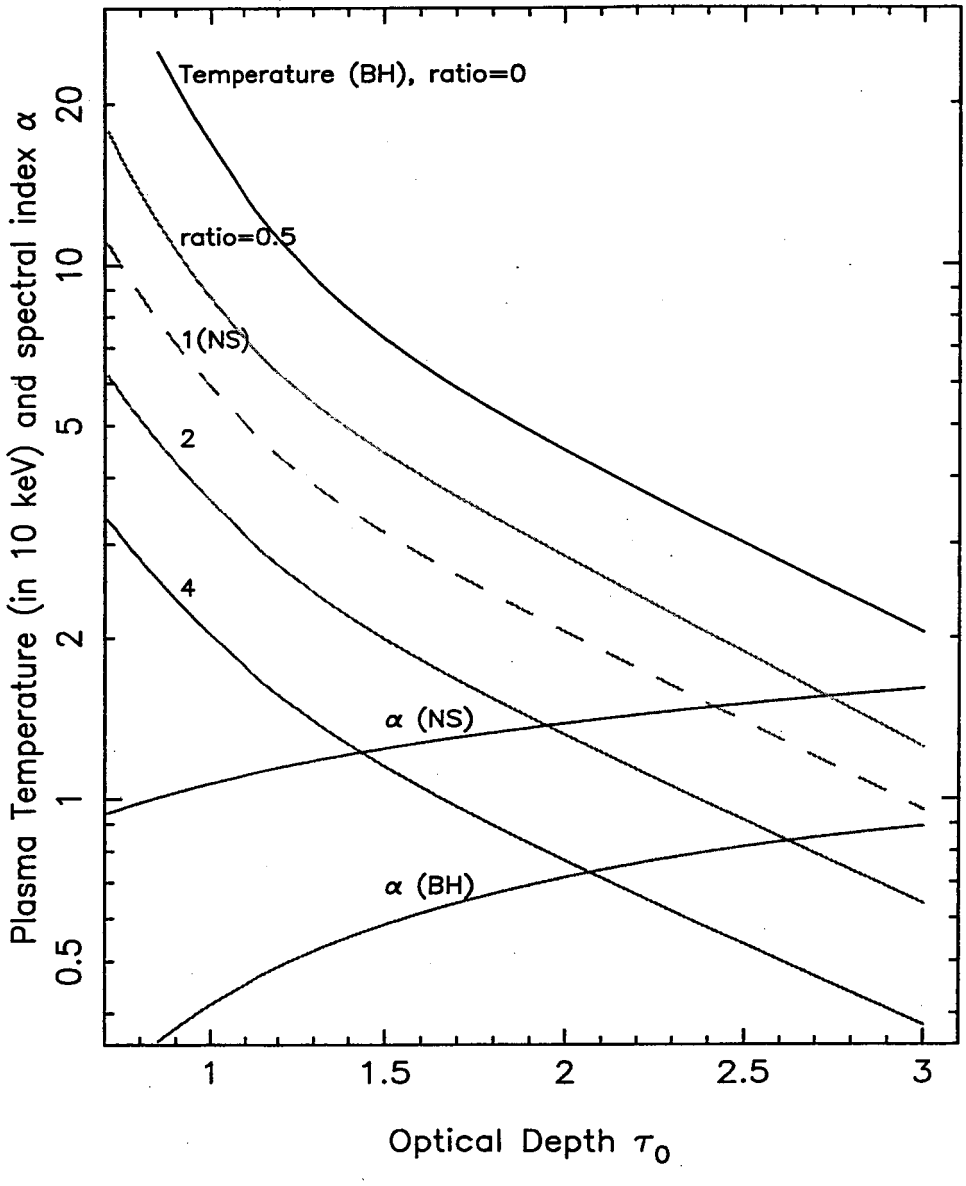

Fig. 5.— Energy spectral index vs the TL optical depth. (Thermal Comptonization case)

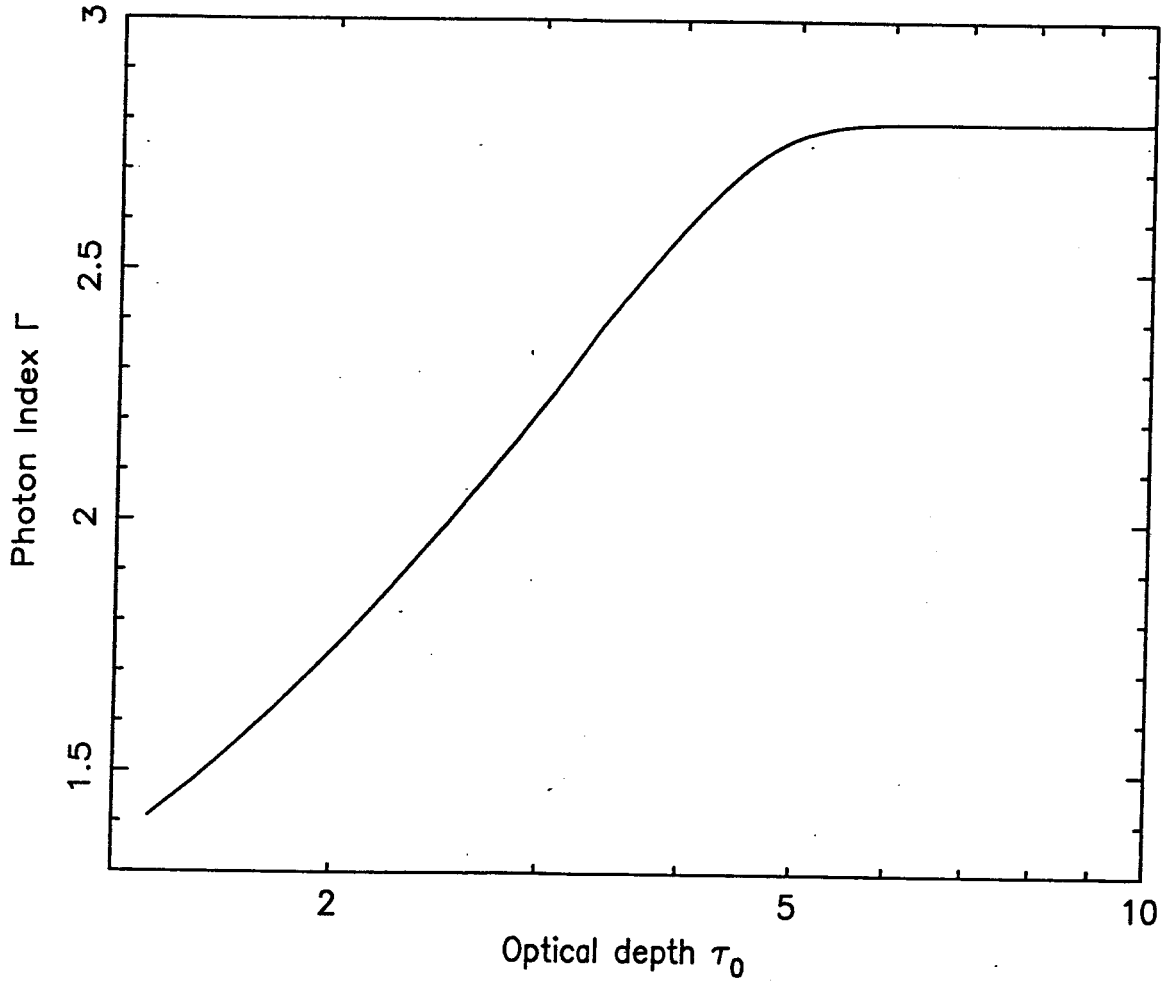

Fig. 6.— Photon spectral index vs the TL optical depth. (General case)

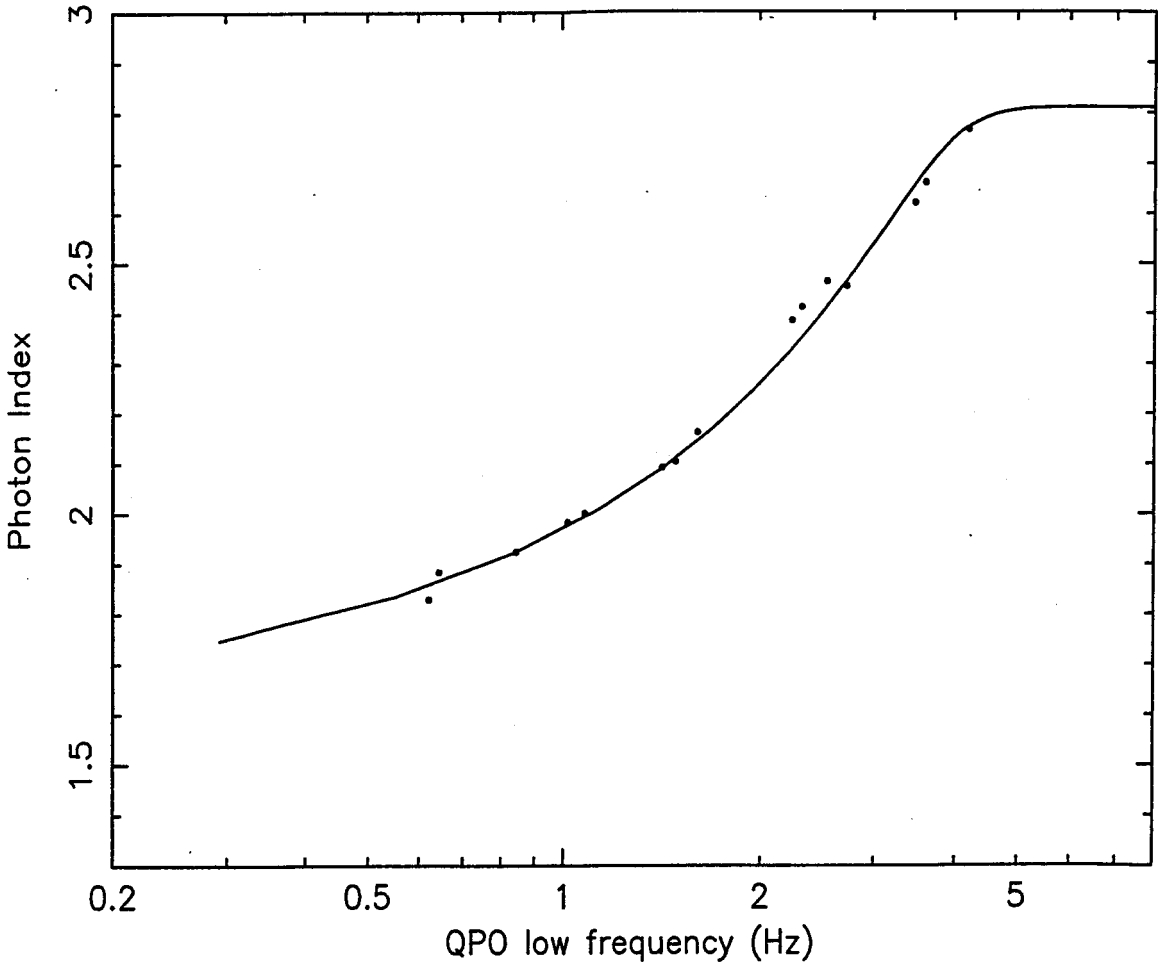

Fig. 7.— Plot of power-law index versus QPO centroid frequency for the plateau observations of GRS 1915+105 from Vignarca et al. 2003 along with a fit using the TL model with $m = 12$ and $\tau_0 = \gamma^{1.25}$.

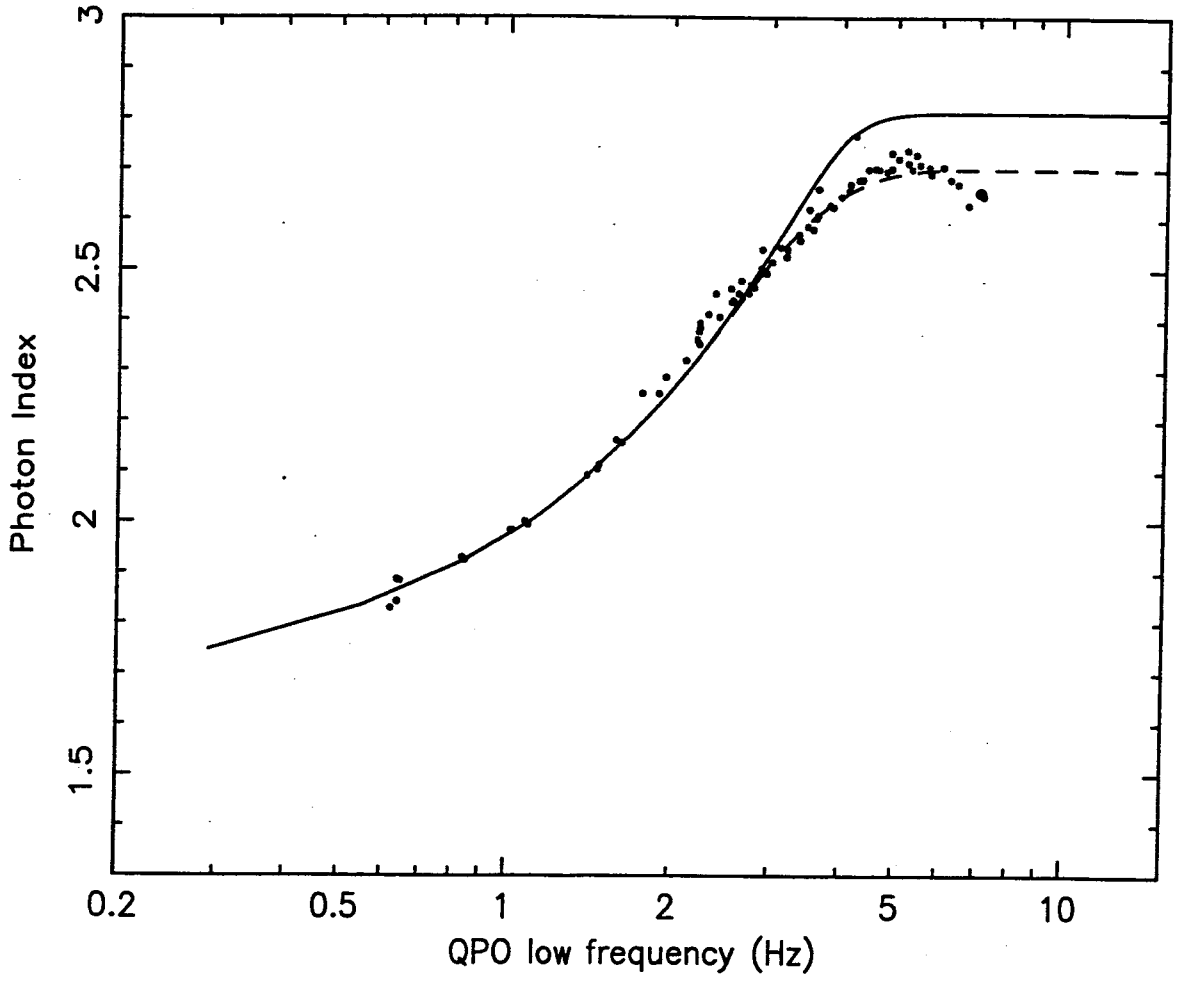

Fig. 8.— Plot of power-law index versus QPO centroid frequency for the observations of class β and ν (black points) and α and ν (red points =obs. 15,16) of GRS 1915+105 from Vignarca et al. 2003 along with a fit using the TL model with $m = 12$ and $\tau_0 = \gamma^{1.25}$. Values for the plauteau observation observations (see previous Figure) are plotted for comparison (blue points).

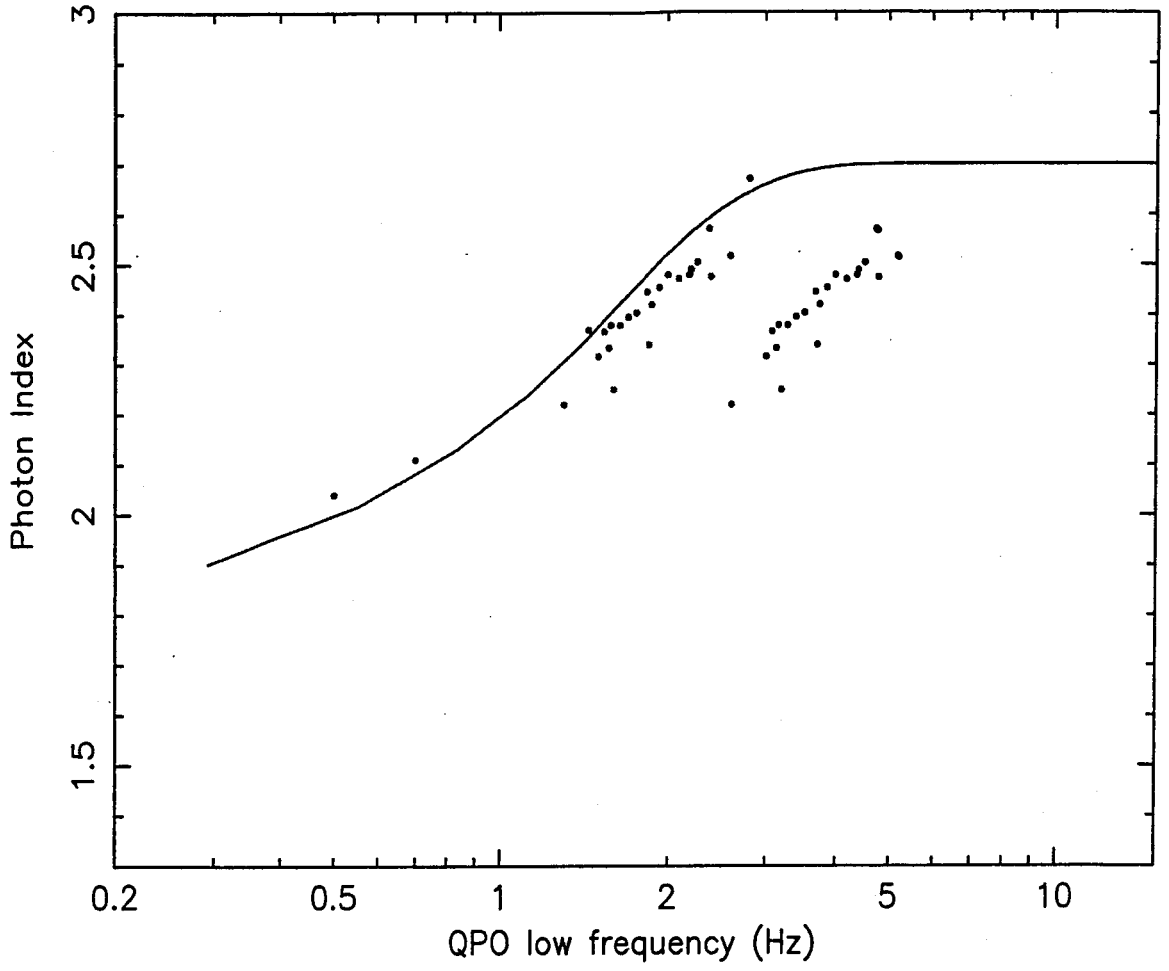

Fig. 9.— Plot of power-law index versus QPO centroid frequency for the observations of class α and ν of GRS 1915+105 from Vignarca et al. (2003) (black points=obs. 18). Blue points correspond to the values for observations by Fiorito et al (2003) (see text). Magenta points correspond to positions where should be points with half of those frequencies. Red points correspond to positions where should be points with half of frequencies for obs. 18 (red points). A curve (blue solid line) is for $m = 12$ and $\tau_0 = \gamma^{1.5}$.

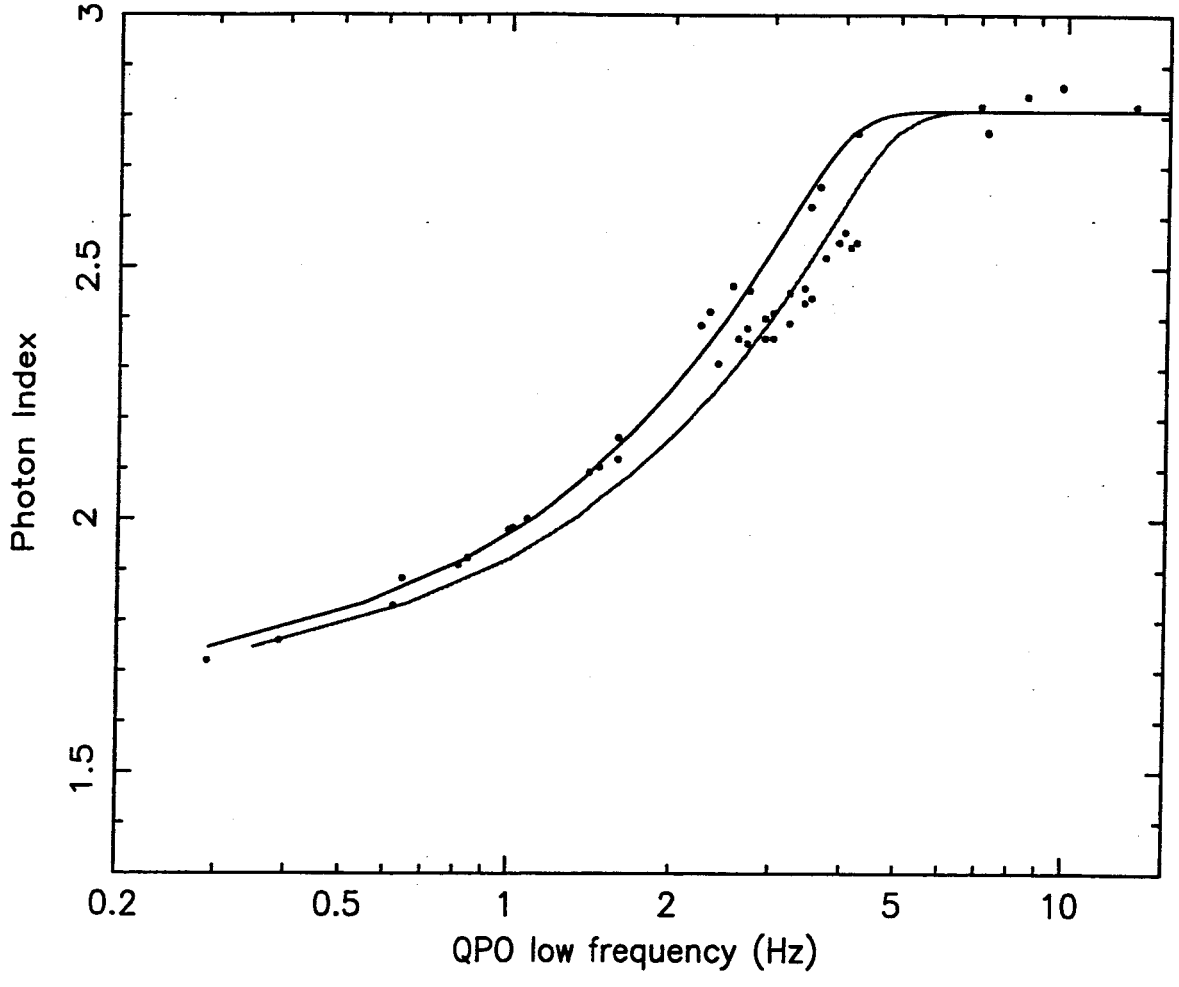

Fig. 10.— Comparison of the observed (Vignarca et al. 2003) and theoretical correlations (solid lines) of photon index vs QPO low frequency between GRS 1915+105 and XTE J1550-564. Black points and line for XTE J1550-564 and red points and line for GRS 1915+105. The XTE J1550-564 curve is produced by sliding the GRS 1915+105 curve along the frequency axis with factor 12/10 (see text for details).

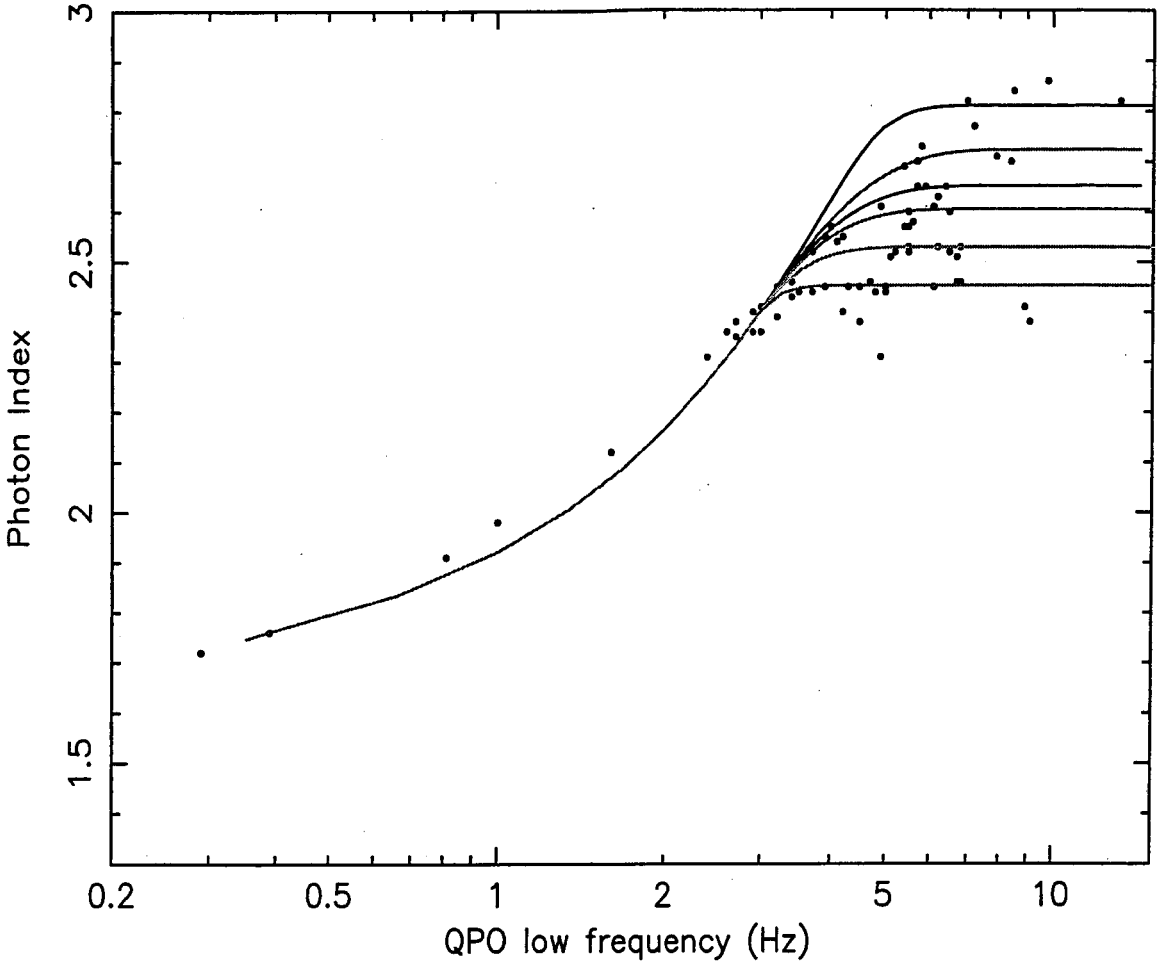

Fig. 11.— Comparison of the observed correlation of photon index vs QPO low frequency for XTE 1550-564 (black points) with the inferred correlation The saturation index value in the theoretical curve is related to specific value of the plasma temperature of the converging inflow kT_{ci}, which changes from 5 keV to 20 kev from the top curve to the bottom respectively.

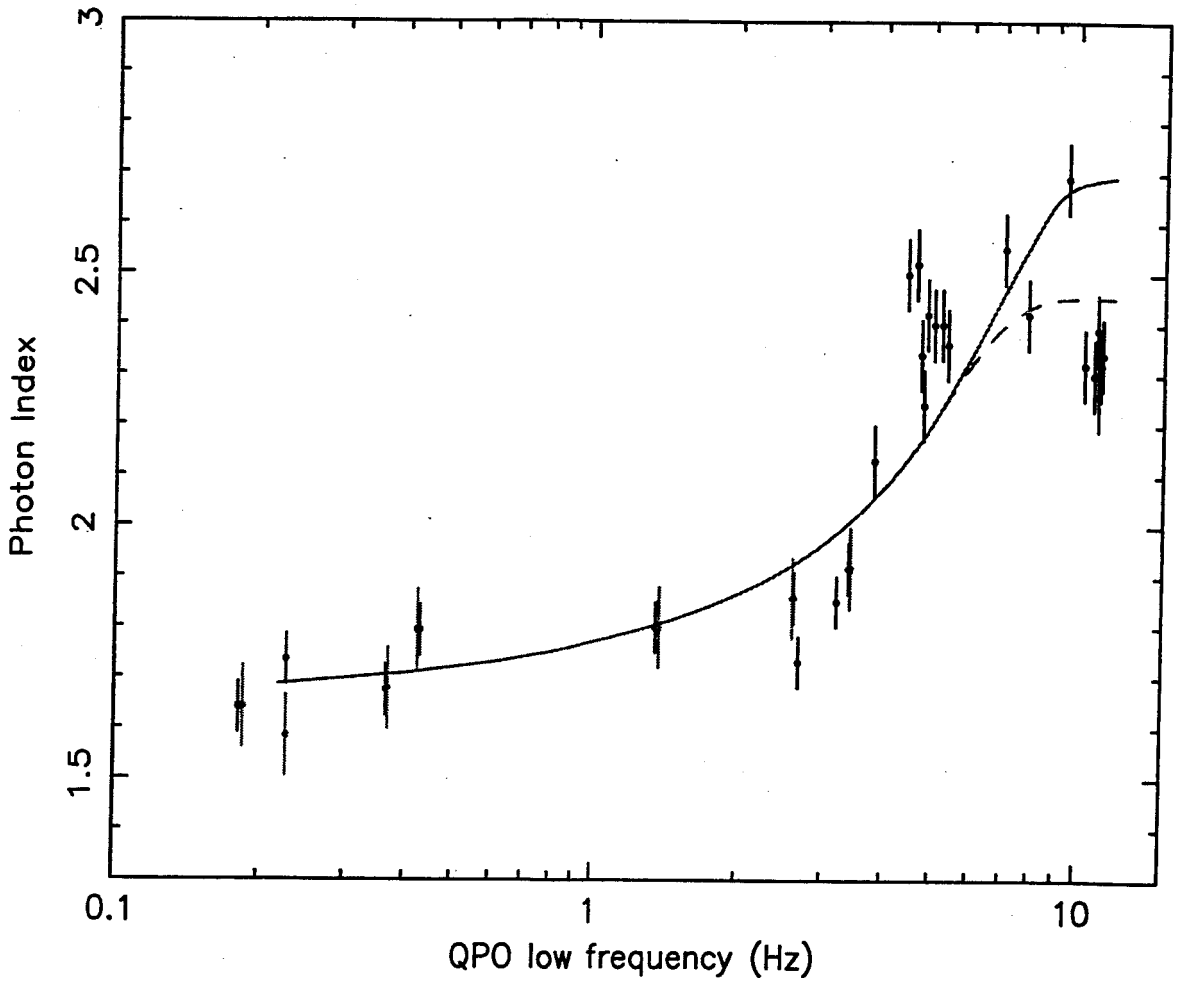

Fig. 12.— Comparison of the observed correlation of photon index vs QPO low frequency with the inferred correlation. Data points are for 4U 1630-47.(see text for details).